TECHNICAL REPORT No. 52

IMPACT OF MODIFIED PHYSICAL PROCESSES ON THE TROPICAL SIMULATION IN THE ECMWF MODEL

by

U.C. Mohanty*, J.M. Slingo and M. Tiedtke

*Visiting Scientist on leave from
Centre for Atmospheric Sciences
Indian Institute of Technology
New Delhi, India

October 1985

Abstract

This paper describes the impact on the tropical simulation in the ECMWF model of various changes to the physical processes within the model. A series of 10 day forecasts were carried out, each integration starting from 12Z on 11 June 1979 and covering the rapid intensification of the Asian summer monsoon over the Arabian Sea and Southern India. The changes to the physical processes involved modifications to the radiation, cloud cover prediction and Kuo convection schemes and the introduction of a shallow convection scheme.

The changes to the convection, particularly the introduction of the shallow convection scheme, are found to have the greatest impact on the tropical circulation and precipitation. There is a marked improvement in the trade winds and in the precipitation associated with the ITCZ. An interesting result of this study is the sensitivity of the monsoon simulation to the combined effects of the radiation and convection changes. It is found that only when the radiation changes are combined with the convection changes is there a marked improvement in the monsoon region. The intensification of the low level flow over the Arabian Sea is then much improved as are the onset of the rains over Southern India and the establishment of the upper level cross equatorial return flow.

C O N T E N T S

1. INTRODUCTION

This report describes the results of a series of 10-day forecasts to assess the model's simulation of the tropical circulation, in particular the onset of the Indian monsoon. In each forecast some aspect of the physical processes was altered and its impact on the model's performance assessed. Each integration started from 12Z 11 June 1979 and covered the rapid intensification of the Indian Monsoon which took place in the subsequent days. Since the initial data already contain the main features of the low level monsoonal flow over the Arabian Sea, the model's ability to represent the observed intensification of the flow is very dependent on its representation of the processes that cause this intensification.

The summer monsoon is associated with the establishment of a low-level (~850mb) westerly jet off the east coast of Africa and the Arabian Sea, called the Somali Jet, and an upper tropospheric (~150mb) easterly jet over the Indian peninsula and adjoining seas, known as the Tropical Easterly Jet (TEJ). These jets are associated with a strong low-level cross-equatorial flow from the Southern Hemisphere (low-level convergence) and an upper tropospheric divergent flow. The onset of the summer monsoon over the Indian subcontinent is marked by:

(a) a rapid intensification of both jets;

(b) intensification of the sub-tropical anticyclone over the Himalayas at about 150mb and shift of the westerly jet to the north of the Himalayas;

(c) an increase of cyclonic vorticity (the so-called 'onset vortex') over the Arabian Sea;

(d) commencement of monsoon rainfall over the south-west coast of India.

Although the mechanism of the onset of monsoon is not well understood, diagnostic studies with FGGE level-IIIb data and the subsequent years operational analyses of ECMWF (Mohanty et al, 1983; Pearce and Mohanty, 1984) indicate that the low-level cross-equatorial flow off the East African coast, in response to the heating over Saudi Arabia, Pakistan and North-West India, leads to an increase in surface moisture flux and moisture content of the atmosphere, reaching a level sufficient to produce deep cumulus convection and latent heat release. This provides an additional heat source in the Arabian Sea and the whole circulation continues to intensify through a positive moisture feed back leading to the onset of monsoon over the Indian subcontinent. This process is characterised by an increase of deep convection over the Arabian Sea, extending into the Bay of Bengal and across peninsular India and leads to the commencement of rainfall over the south west coast of India and Sri Lanka.

Further, the results of the FGGE intercomparison experiments (Krishnamurti et al, 1983) and numerical simulation results from FGGE data by a number of investigators (e.g. Krishnamurti and Ramanathan, 1982; Mohanty et al, 1984) indicate that the intensification of the monsoon flow is mainly dictated by release of convective instability and is very sensitive to the intensity and location of the diabatic heating in the troposphere.

Although the representation of convective processes is clearly important, the development and release of convective instability is also dependent on other aspects of the physical parameterisations, particularly the radiative cooling and the vertical fluxes of heat and moisture from the surface, through the boundary layer.

In this series of experiments the changes to the parameterisation schemes involve other aspects of the physical processes. These changes will be described and their general effects on the forecast will be briefly discussed. The impact of these changes on the tropical circulation and precipitation will be considered in more detail. Special emphasis will be placed on the development of the Indian Monsoon.

2. DESCRIPTION OF THE EXPERIMENTS

2.1 Model description

The integrations were performed with the ECMWF T63 spectral model (Simmons and Jarraud, 1984). The model has 16 levels in the vertical based on a hybrid coordinate system (Fig. 1). The model includes a comprehensive set of physical processes based on those described by Tiedtke et al (1979).

2.2 Description of modified parameterisation schemes

(a) Modified Kuo scheme

In the tropics (30°S-30°N) various modifications have been made to the Kuo convection scheme. Firstly the cloud base is redefined as the condensation level for near surface air rather than that for air with the mean characteristics of the well mixed layer. This change enhances the occurrence of cumulus convection and gives a more realistic response, by the convection, to the diurnal cycle in surface heating of the tropical land masses. The second important change involves the moistening parameter β:

$$\beta = 1 - \frac{\int_{p_{top}}^{p_{base}} RH \, dp}{p_{base} - p_{top}}$$

where P_{top} and P_{base} are the pressures of the top and base of the cloud. In its original form it tends to over moisten the environment and to underestimate the latent heat release. In the modified code the moistening parameter is replaced by β^3 which, with its stronger dependency on the environmental saturation deficit, gives less moistening and more heating. Two other minor changes involve simplification of the code with removal of the ice phase and of the possibility for multi-layered cumulus convection. The net effect of all these changes is to give a much improved structure in convective situations. An example of this can be seen in Fig. 2 with a typical ascent over West Africa. With the original Kuo scheme (Fig 2(b)) the tendency to produce states that are too cold and too moist is clearly evident.

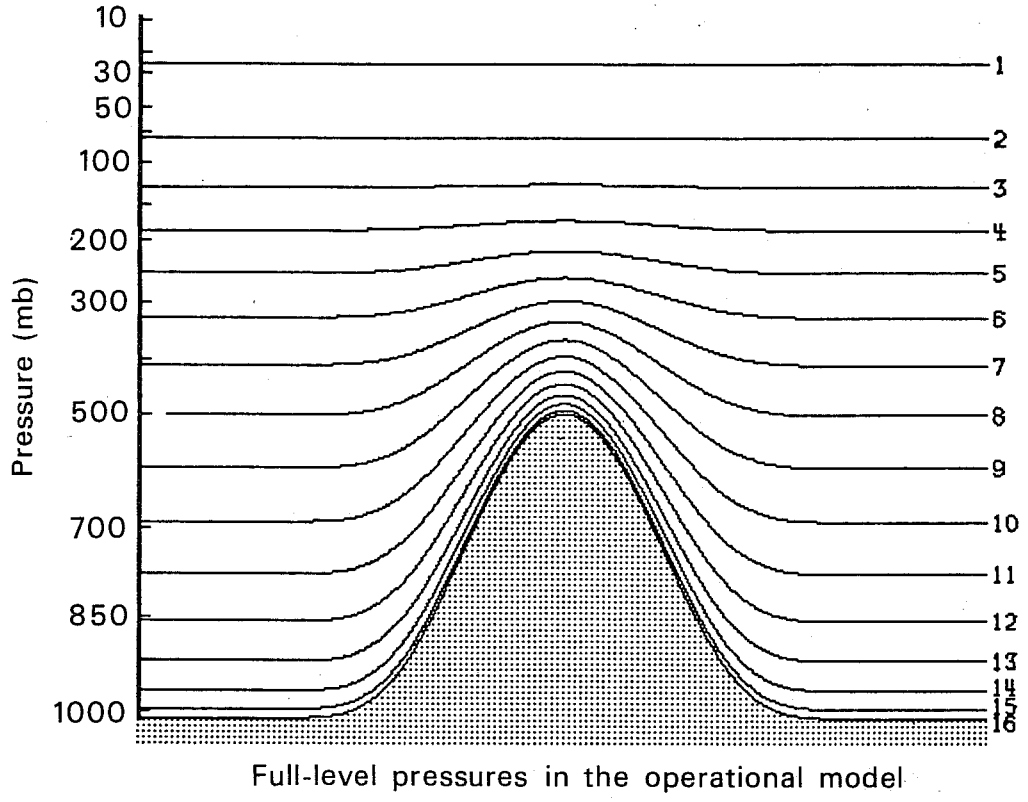

Fig. 1 Vertical hybrid coordinate system of the operational model.

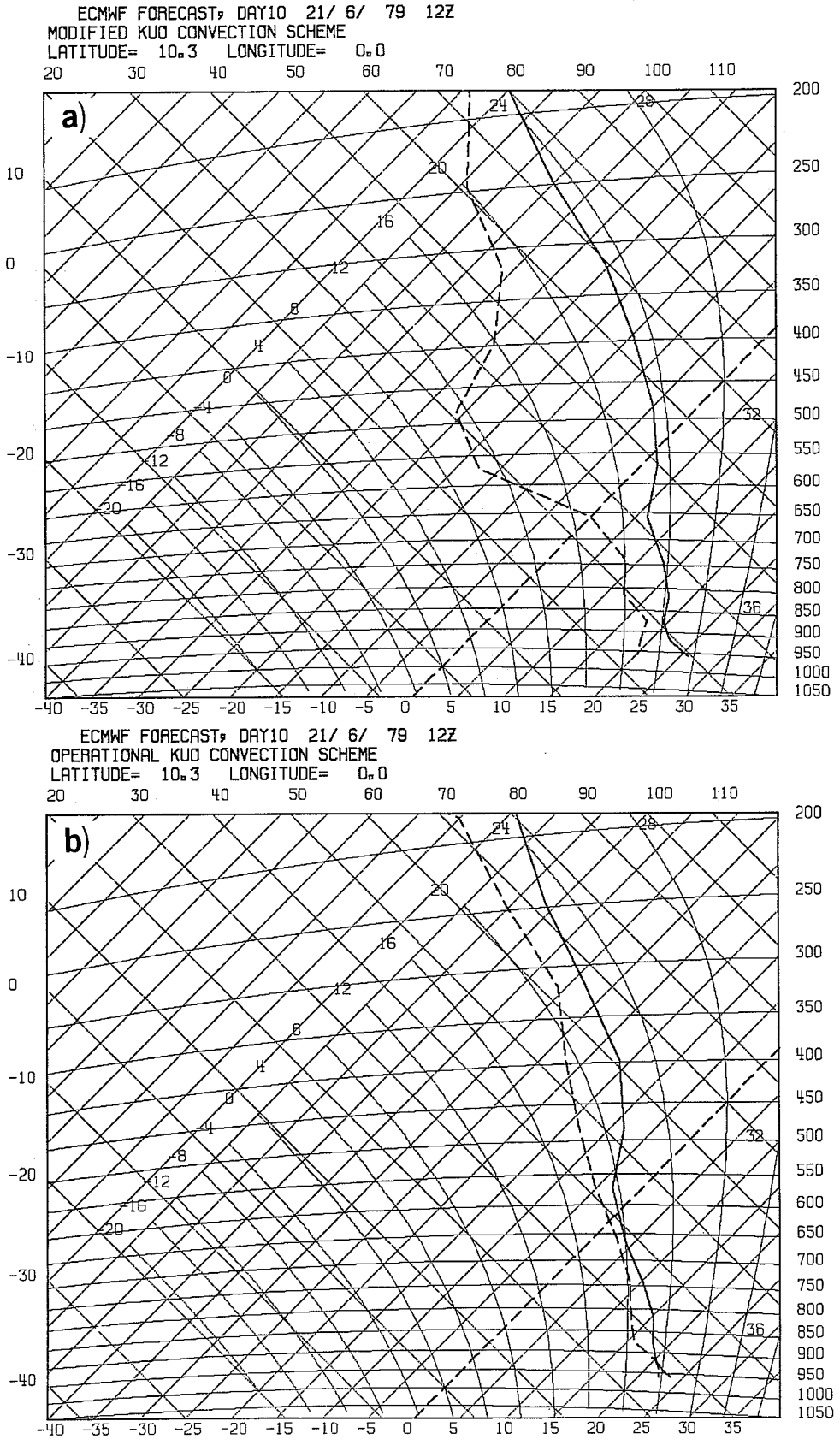

Fig. 2 Vertical distributions of temperature and dew point at day 10 for a grid point over W. Africa (10°N, 0°E)
(a) Modified Kuo scheme
(b) Original Kuo scheme.

With the modified scheme (Fig. 2(a)) the middle and upper troposphere is considerably warmer and drier due mainly to the redefined moistening parameter.

(b) Shallow convection

A parameterisation scheme for shallow convection has been developed in which the turbulent transports of sensible heat and moisture are represented by vertical diffusion within moist convectively unstable layers, through cloud base and through the level of non-buoyancy. A full description of the scheme and a preliminary assessment is given in Tiedtke (1985). The scheme effectively transports moisture from the boundary layer into a cloud layer above. This is most pronounced in the trades, where shallow convection counteracts the drying and warming effect of the mean subsidence. Typical profiles in the trade winds (Fig. 3) show that with shallow convection the well mixed boundary layer is topped by a cloud layer (Figs. 3(a) and 3(c)) which is lacking without shallow convection (Fig 3(b) and 3(d). The cloud layer extends over several model layers and the depth of the total moist layer (boundary layer + cloud layer) is considerably deeper.

(c) Revised infrared radiation scheme

The original ECMWF radiation scheme was based on a two-stream approximation of the radiative transfer equation both in the solar and infrared parts of the spectrum (Geleyn and Hollingsworth, 1979). In both wave domains an effective absorber path length method (EAM) was used to incorporate the effects of gaseous absorption and emission. This method works well in the shortwave but the approximations that are necessary in the longwave to make the scheme computationally viable have led to problems in particular with the treatment

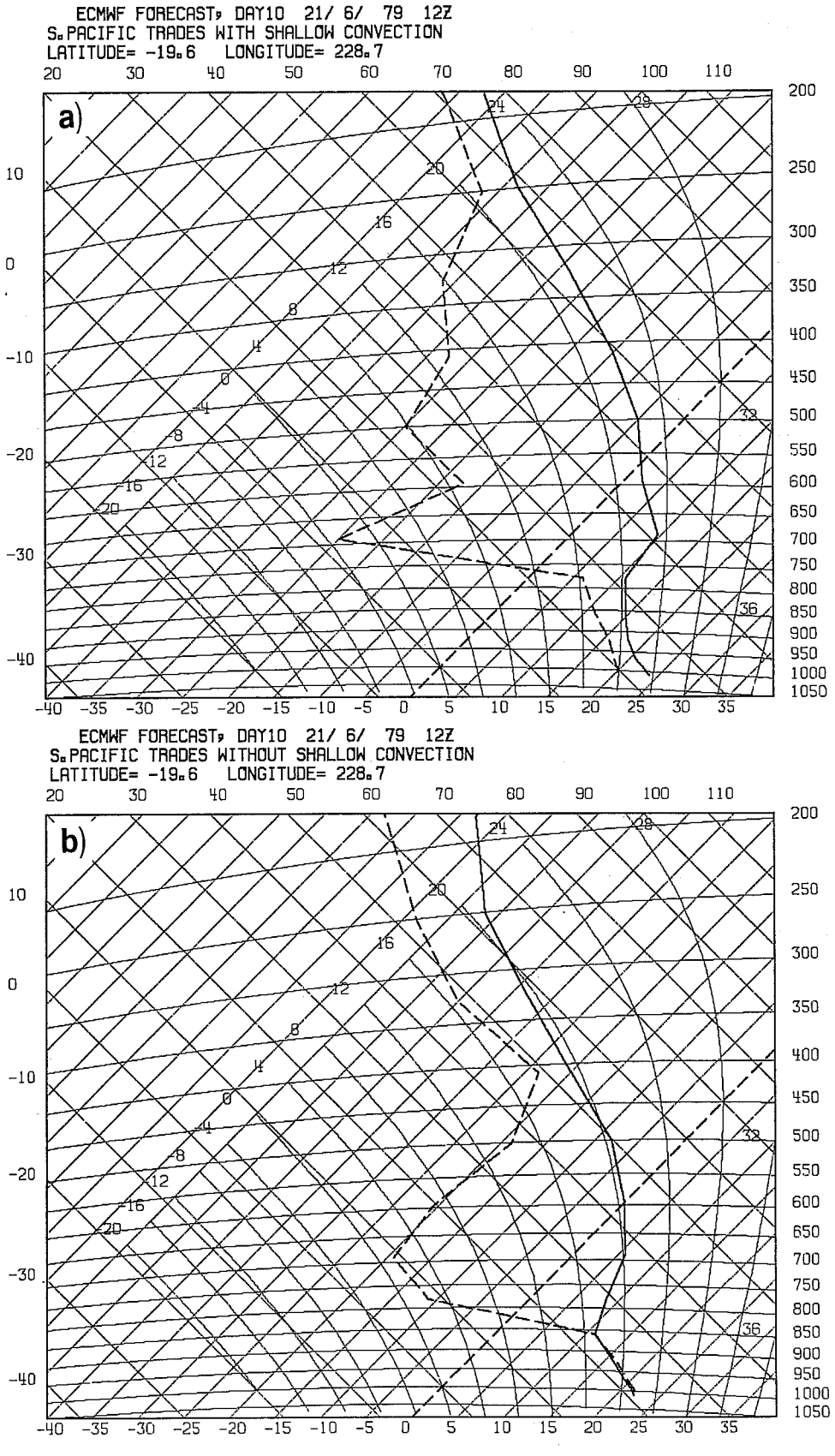

Fig. 3 Vertical distributions of temperature and dewpoint at day 10 for 2 grid points over the S. Pacific (20°S, 130°W; 20°S, 100°W)
(a) and (c) with shallow convection,
(b) and (d) without shallow convection.

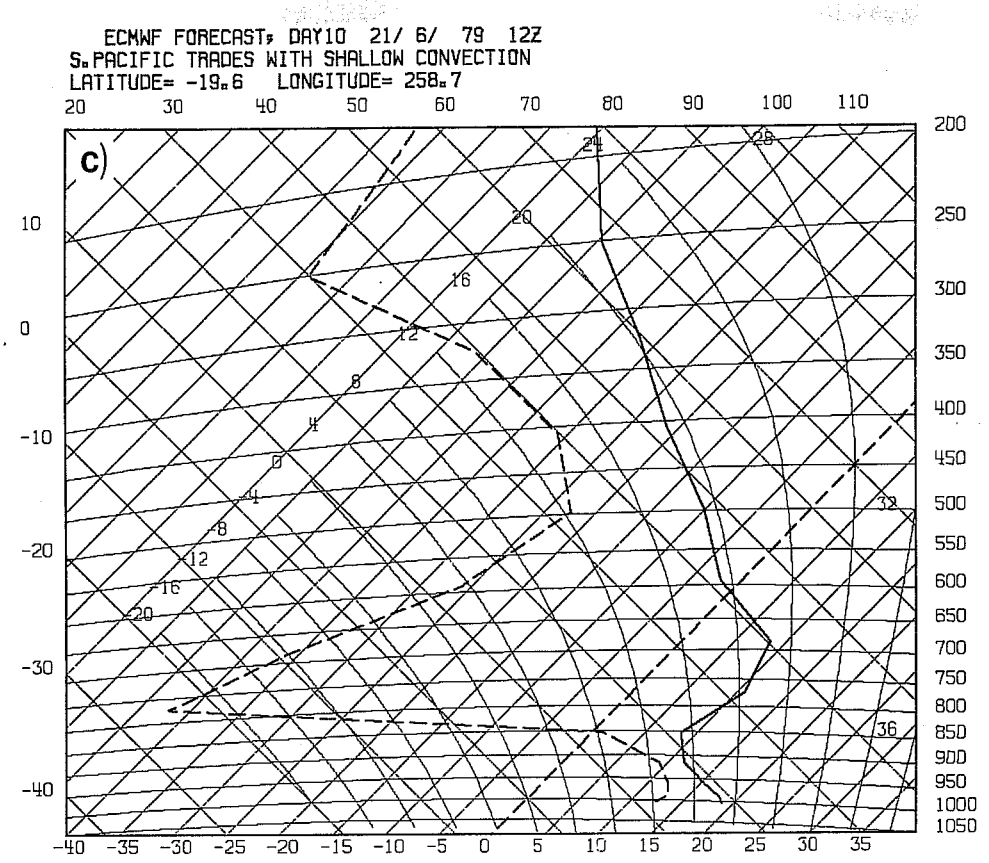
ECMWF FORECAST, DAY10 21/ 6/ 79 12Z
S.PACIFIC TRADES WITH SHALLOW CONVECTION
LATITUDE= -19.6 LONGITUDE= 258.7
c)
20 30 40 50 60 70 80 90 100 110
10 0 -10 -20 -30 -40
200 250 300 350 400 450 500 550 600 650 700 750 800 850 900 950 1000 1050
-40 -35 -30 -25 -20 -15 -10 -5 0 5 10 15 20 25 30 35

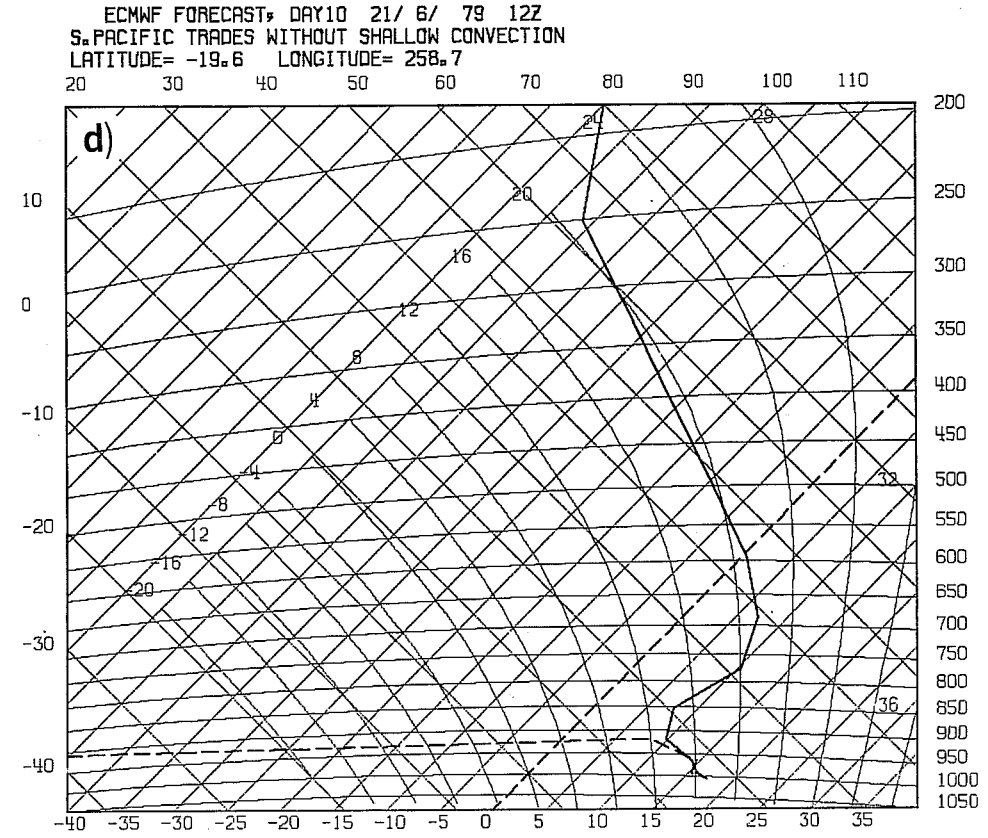
ECMWF FORECAST, DAY10 21/ 6/ 79 12Z
S.PACIFIC TRADES WITHOUT SHALLOW CONVECTION
LATITUDE= -19.6 LONGITUDE= 258.7
d)
20 30 40 50 60 70 80 90 100 110
10 0 -10 -20 -30 -40
200 250 300 350 400 450 500 550 600 650 700 750 800 850 900 950 1000 1050
-40 -35 -30 -25 -20 -15 -10 -5 0 5 10 15 20 25 30 35

Fig. 3 (contd.)

of the emission terms in the atmosphere. The scheme gives excessive cooling rates in layers with small amounts of scatterer due to clouds and aerosols (Slingo, 1982). To overcome this problem a longwave radiation scheme with a revised treatment of gaseous absorption has been developed. This is based on the technique of exponential sum fitting (ESFT) in which the gaseous transmission function is approximated by a series of decaying exponentials. Each exponent behaves like a monochromatic optical depth which can be easily incorporated into the multiple scattering form of the existing radiation scheme. A computationally efficient version of this method (FESFT) which simplifies the treatment of gaseous overlap has been developed (Ritter, 1984). This scheme gives a much more realistic response to small amounts of cloud as can be seen in Fig. 4. The EAM scheme exhibits a strong cooling near 600 mb even though the corresponding cloud cover is small; it also underestimates the cooling near the surface associated with the rapid increase in humidity. The FESFT scheme replaced the EAM scheme in the operational model on 4 December 1984.

(d) New cloud scheme

A new cloud prediction scheme has recently been developed and was implemented in the operational model on 1 May 1985. It replaces a scheme which was based on relative humidity with the restriction that no clouds were allowed in the well-mixed layer (Geleyn, 1981). Four shortcomings of the scheme were too many deep clouds, too little tropical cirrus, too little subtropical cloudiness and poor representation of the diurnal variation in cloudiness (Slingo and Ritter, 1985). The new scheme is intended to rectify these faults.

The new scheme is based on a diagnostic approach in which the cloudiness is predicted empirically from model variables, the functions chosen to represent the probability of cloud occurring under certain atmospheric conditions. The

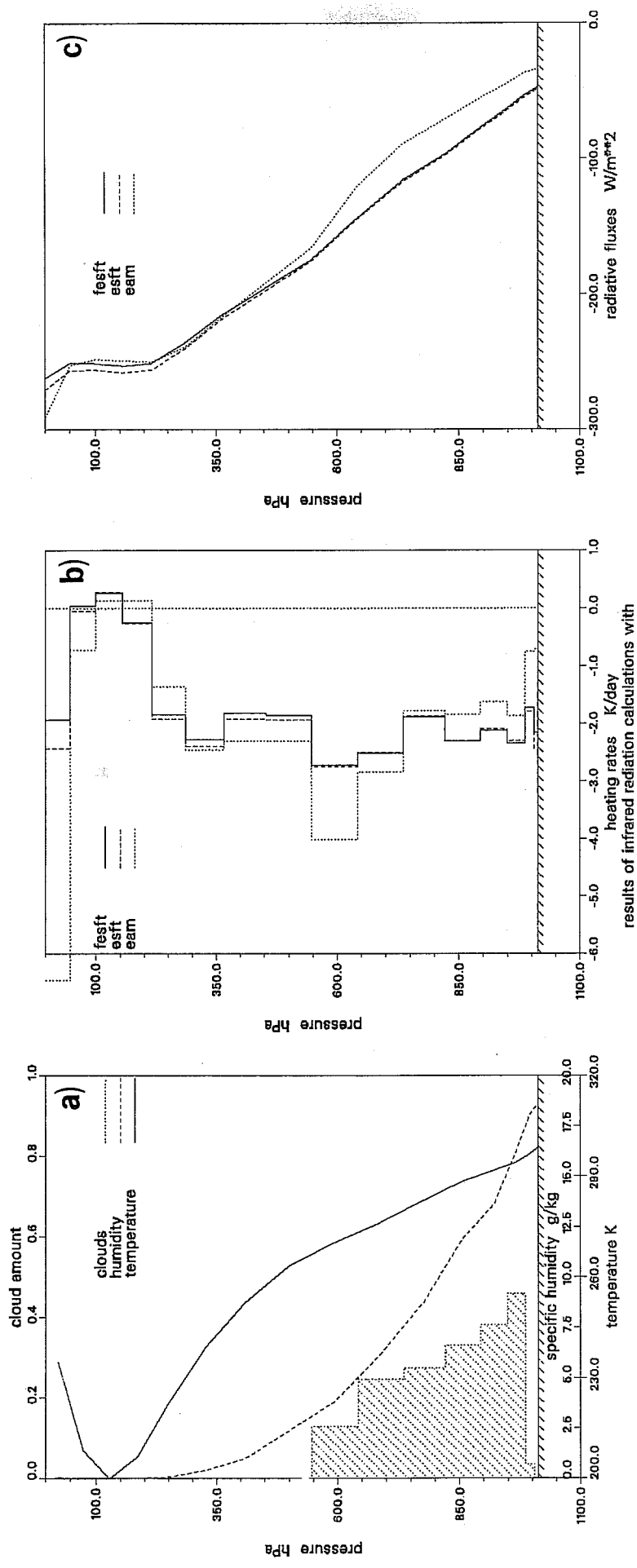

Fig. 4 Effect of changes to the radiation code on the vertical profiles of infrared radiative cooling rates and net fluxes.

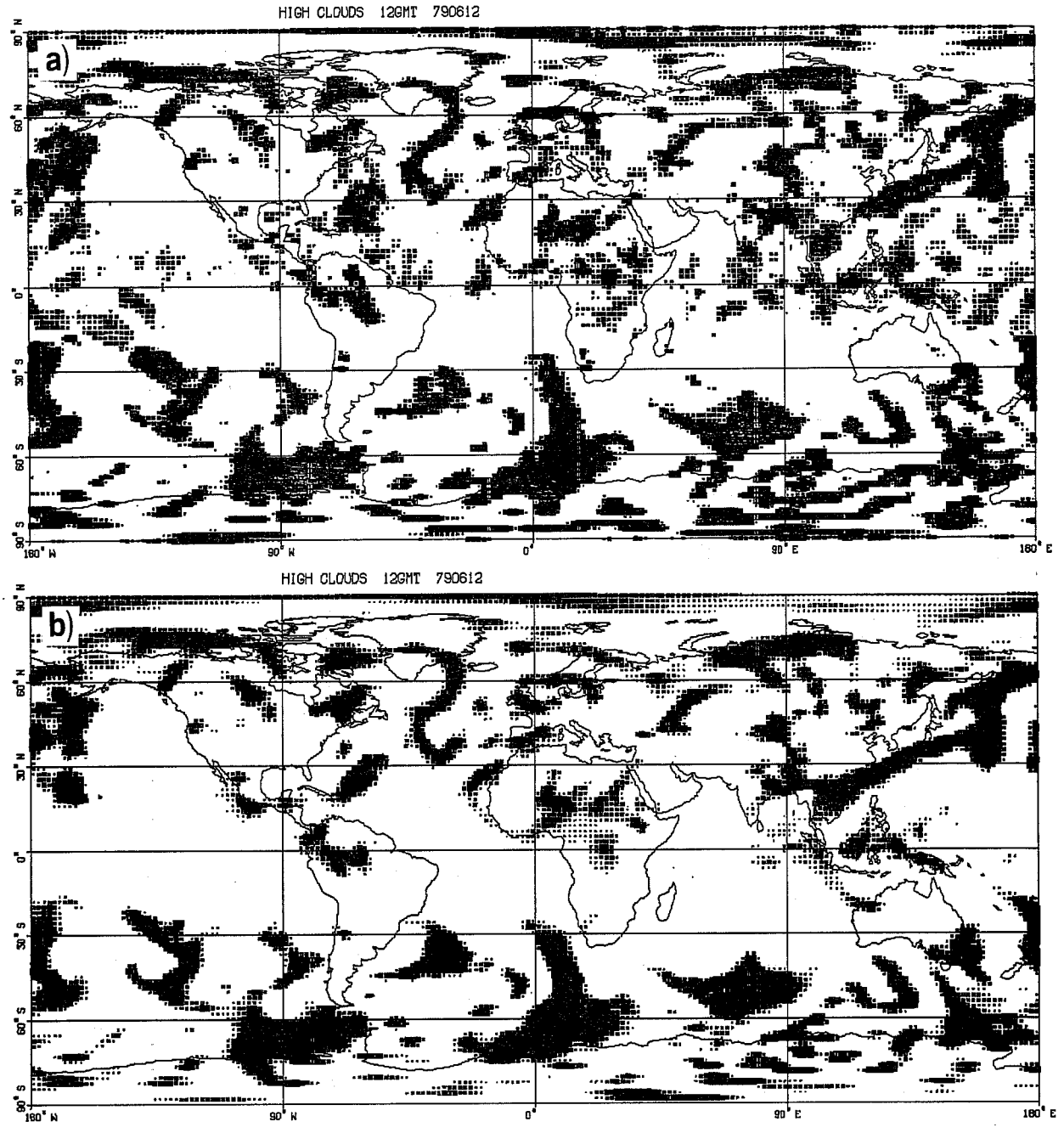

Fig. 5 Distribution of high cloud for day 1 of a forecast from 11 June 1979 (a) new scheme (b) original scheme.

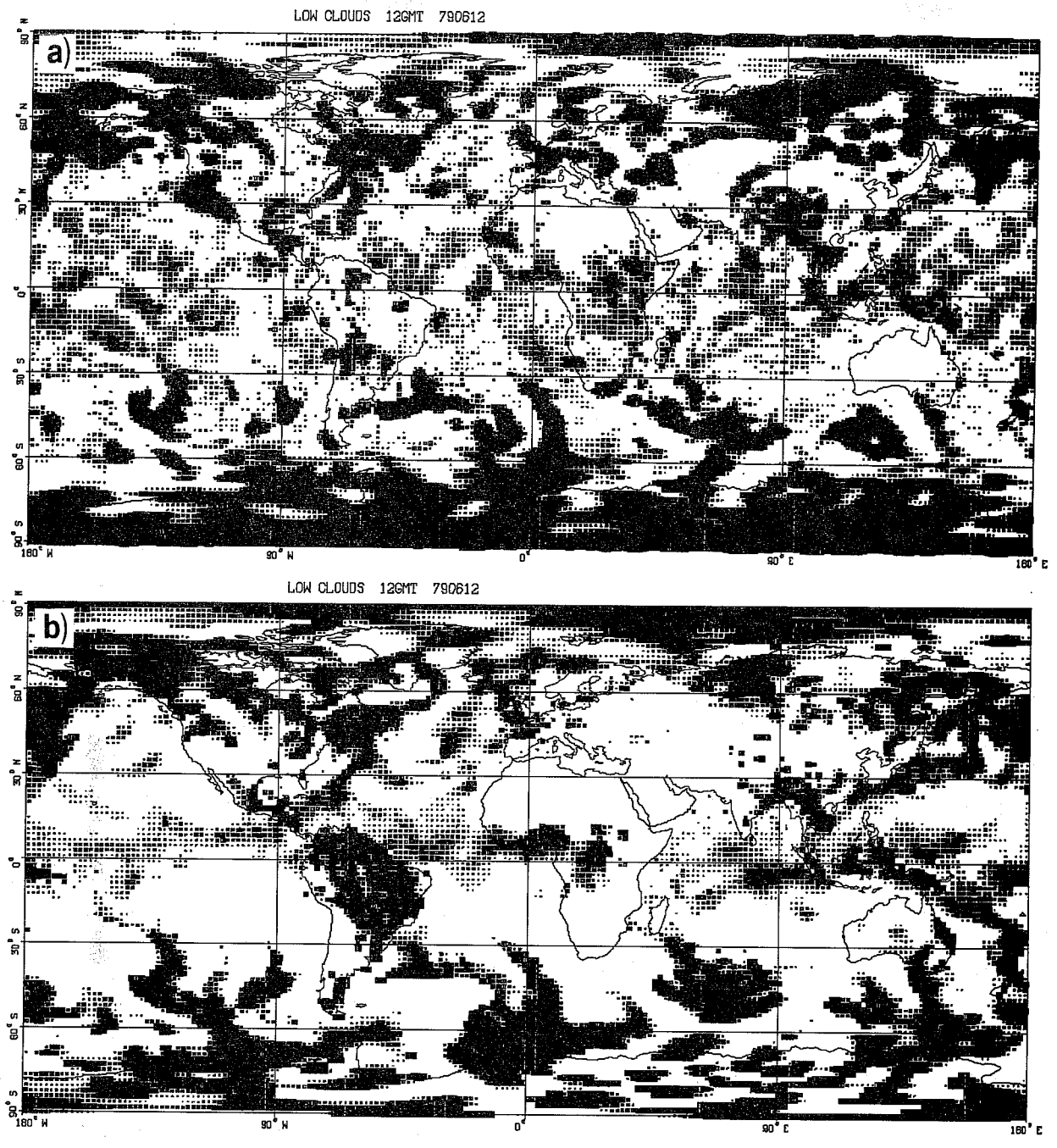

Fig. 6 As Fig. 5 for low-level clouds (cumuliform + stratiform clouds for new scheme).

scheme will be described briefly here but a fuller discussion of its development and assessment of its performance is given in Slingo (1985). Four parameters are used for diagnosing cloudiness - convective activity, relative humidity, vertical velocity and atmospheric stability. The scheme allows for four cloud types - convective and three layer clouds (high, middle and low level). High (cirrus) clouds are derived from relative humidity (frontal and extratropical cirrus) and convective activity (anvil cirrus). Middle level clouds are based solely on relative humidity. Convective clouds are derived from a logarithmic function of the time-averaged precipitation rate from the model's convection scheme. Convective cloud base and top are also supplied from the convection scheme. Low level stratiform clouds are divided into two classes; those associated with extratropical fronts and tropical disturbances and those that occur in relatively quiescent conditions and are directly associated with the boundary layer. The first class of clouds are characterized by generally moist air and large scale ascent. These are parameterized using relative humidity and vertical velocity. The second class of low level clouds are strongly linked to the boundary layer and are invariably associated with low level inversions in temperature and humidity, e.g. tradewind inversion. These are parameterized using the strength of the inversion and the relative humidity at the base of the inversion. With this, the persistent clouds off the western seaboards are well represented as are the summertime Arctic stratus clouds and those over the cold waters of the North Pacific.

The scheme has been tested in a variety of cases and seems to give realistic cloud distributions. It also gives a small but consistent improvement in the model's performance. In Figs. 5 and 6 the high and low level cloud distributions from the new scheme are compared with those from the operational scheme for day 1 of the forecast from 12Z 11 June 1979. The new scheme shows

a marked improvement in the tropics with cirrus being predicted in the Atlantic and off South America. The high clouds over the Indian Ocean, heralding the onset of the monsoon, are also captured by the new scheme. Fig. 6 shows a marked increase in the low level cloudiness over the subtropics with the new scheme and the transition from the dense frontal clouds of the extratropics to the broken convective regimes of the tropics is striking. In particular, the scheme has been successful in capturing the areas of subtropical low level cloudiness off the western seaboards of the major continents. The representation of the diurnal cycle in cloudiness is much improved with the new scheme. Over the tropical continents the cloudiness increases during the daytime and decreases again as night falls and convection ceases.

2.3 Initial conditions and experiments

All integrations start from real data from the FGGE observing period. A starting date of 12Z 11 June 1979 was chosen so as to cover the period of rapid intensification of the monsoonal flow over India. The fields are analysed and initialised as described by Lorenc (1981) and a data assimilation started from 5 June 1979 using the revised system as described by Lönnberg and Shaw (1983).

The results from five experiments are described - one control and four integrations in which some aspect of the physics was changed. Table 1 gives a list of the experiments and indicates which part of the physics was modified. If no change is indicated then the operational counterpart is used.

Table 1 Experiments and modifications to the physical processes

Experiment	Modified Kuo plus shallow convection	New Radiation	New Clouds
W81 (Control)	-	-	-
X20	X	-	-
X31	-	X	-
Y68	X	X	-
U41	X	X	X

3. RESULTS

3.1 Forecast verification in the tropics

In this section the general performance of the model in the tropics will be considered and the impact of the changes in the physics on the systematic errors will be discussed. Fig. 7 shows the time evolution of the root mean square wind errors at 850mb for the tropical belt (35°S - 32.5°N). The graphs include persistence so that the skill of the forecasts can be assessed. As can be seen the control experiment (W81) develops some substantial errors by the end of the forecast both in the total field and for the very long waves (1-3) where it is worse than persistence for most of the forecast. The introduction of the improved longwave radiation scheme (X31) gives an improvement in the total errors but a lesser change for the very long waves (Fig. 7a) particularly towards the end of the forecast. In comparison the introduction of the shallow convection and modified Kuo schemes (X20) gives only a small improvement in the total errors but has a dramatic effect on the large scale flow (Fig. 7(b)). It is interesting to note that the full benefits of the convection changes are only realised when they are combined with the radiation changes (Y68). Then the errors decrease still further so that the forecast is better than persistence throughout (Fig. 7(b)). The addition of the new cloud scheme with the other changes (U41) gives a further systematic improvement (Fig. 7(a)) so that the best results are obtained when all the changes to the physics are incorporated.

Fig. 7 shows that the model responds quite rapidly to the changes in the physics. By day 4 the effect of the shallow convection and modified Kuo (X20 vs. W81) is already established (Fig. 7(b)). The radiation changes are also

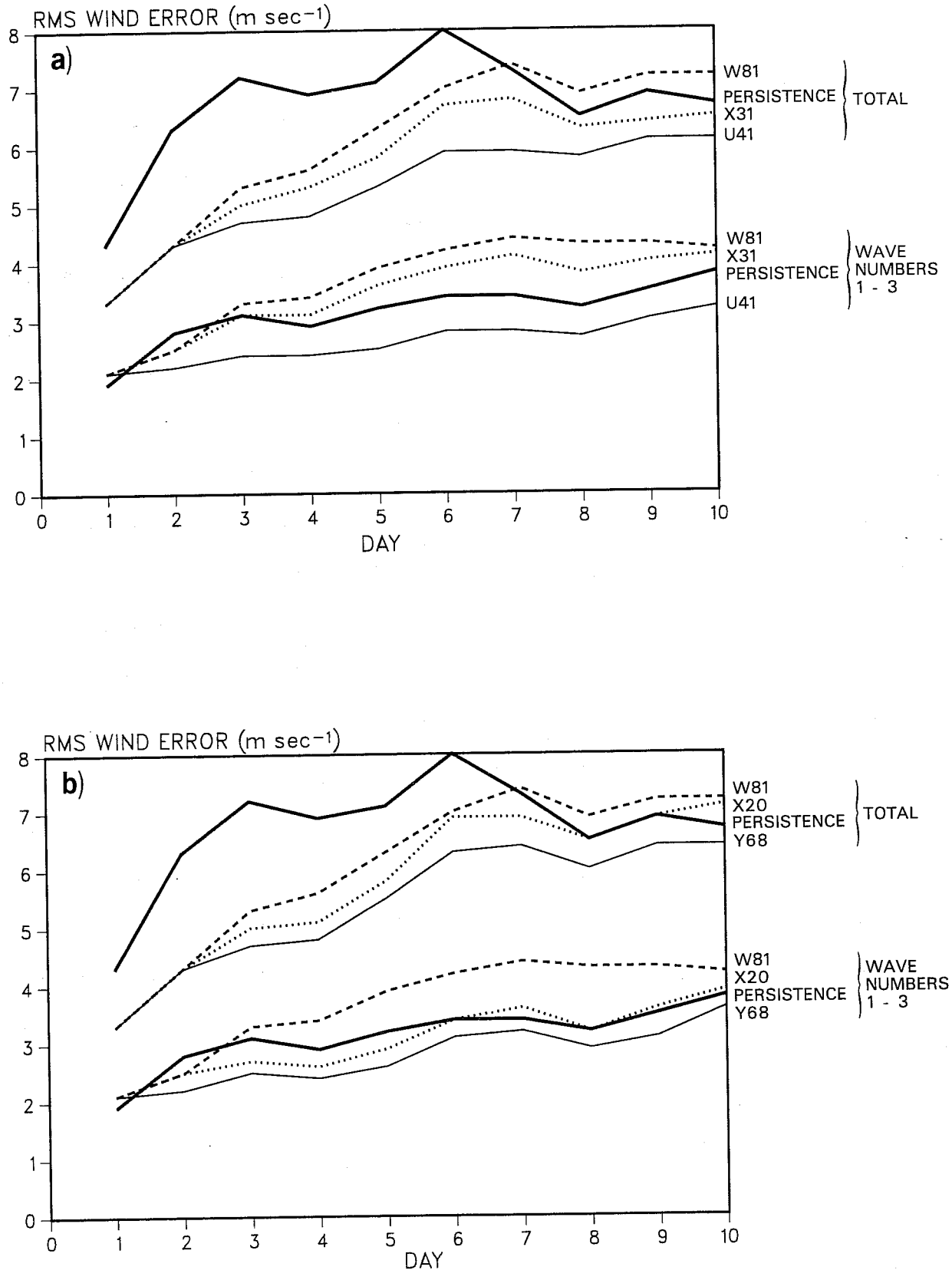

Fig. 7 Time evolution of the root mean square wind errors at 850mb for the tropical belt (35°S - 32.5°N).

evident by day 4 but a further response can also be seen later in the forecast (X31 vs. W81; Y68 vs. X20). The same is true for the new cloud scheme (U41 vs. Y68) and is consistent with the longer time scales of radiative processes.

In order to see what these root mean square errors mean in terms of the flow patterns simulated by the model, the winds at 850mb and 200mb for days 5-10 average (Figs. 8 and 9) were studied. For clarity they are expressed as a difference from the analysed field for the same period which is also shown at the bottom of each figure. At 850mb (Fig. 8) the control experiment (W81) shows the spurious westerly flow over Africa which is a typical feature of operational forecasts, and a rather weak Somali jet. With the introduction of the shallow convection and modified Kuo (X20) the dramatic improvement in the large scale flow, evident in Fig. 7(b), is seen in the strengthening of the trade winds, particularly over the Atlantic and the removal of the spurious westerlies over Africa. The monsoonal flow, however, is still not well simulated. It is only when the convection changes are combined with the radiation changes (Y68) that there is a substantial improvement in this feature. The monsoonal flow is further strengthened with the new cloud scheme (U41). It should be emphasised that in general the shallow convection and modified Kuo schemes improve the low-level tropical circulation to a far greater extent than the radiation changes. The same result is evident in the winds at 200mb (Fig. 9): the spurious equatorial easterly flow across Africa and the Atlantic being largely removed by the convection changes (X20, Y68) but not by the radiation changes (X31). Again the best results are obtained when all the changes are incorporated (U41).

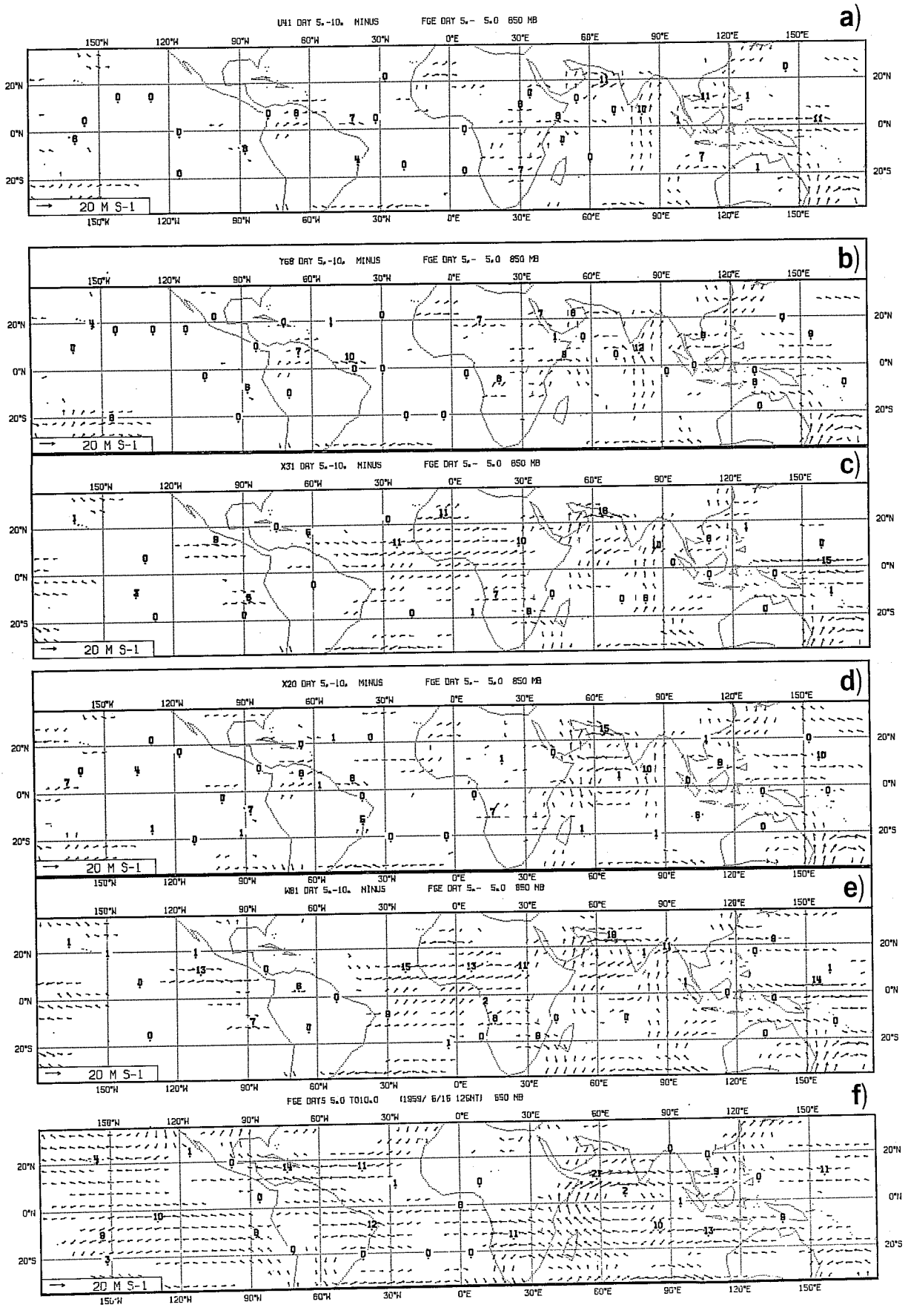

Fig. 8 5-10 day mean tropical flow at 850mb. For the experiments the flow is expressed as the difference from the analysed field.

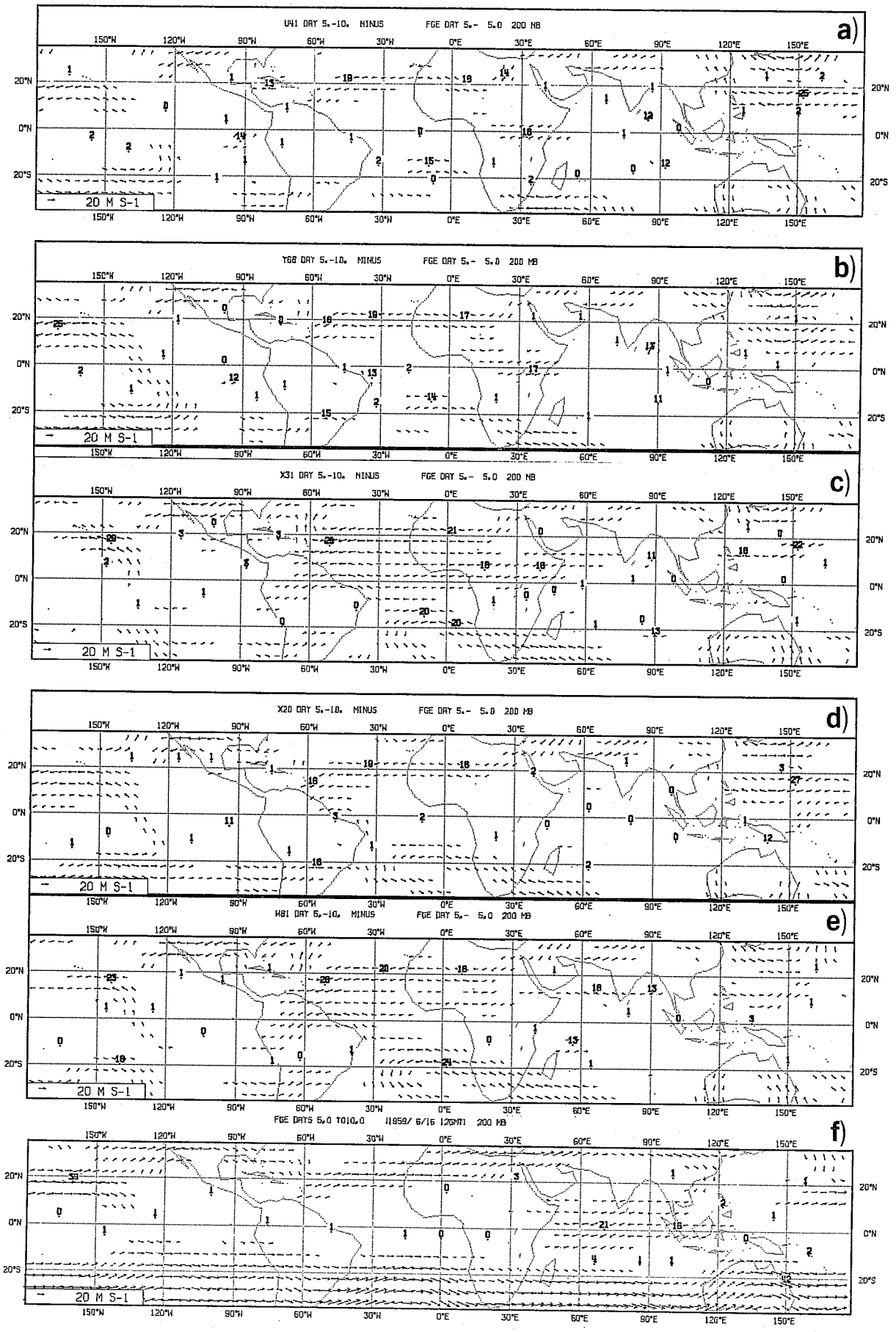

Fig. 9 As Fig. 8 for the mean flow at 200mb.

The convection changes also have a marked impact on the systematic temperature errors of the model (Fig. 10). The model's tendency to generate too cold a tropical and subtropical troposphere (W81; X31) is removed when the convection changes are introduced with a relative warming of about 2K (X20; Y68) associated with an intensified hydrological cycle. The radiation changes alone (X31) reduce the cooling somewhat in the middle troposphere and remove the spurious warming at the troposphere. There is however an increased warming in the stratosphere due to the removal of anomalous longwave radiative cooling which was the result of approximations within the original radiation code. The reduction in cooling in the middle troposphere is a direct result of the more realistic response of the new radiation code to small amounts of cloud as described in 2.2. The increased radiative cooling in the lower troposphere is evident in the temperature errors (X31) and arises from the new scheme's increased, but more realistic, sensitivity to humidity. This cooling is exaggerated by the model's too moist boundary layers in the absence of shallow convection. When shallow convection is included (Y68) the lower tropospheric temperature errors are reduced.

The introduction of the new cloud scheme (U41) leads to a further slight warming in the middle troposphere and slight cooling in the lower troposphere. These changes are related to the different vertical distribution in cloudiness and hence radiative cooling. The original cloud scheme gave too many deep clouds and underestimated the boundary layer cloudiness, particularly in the subtropics.

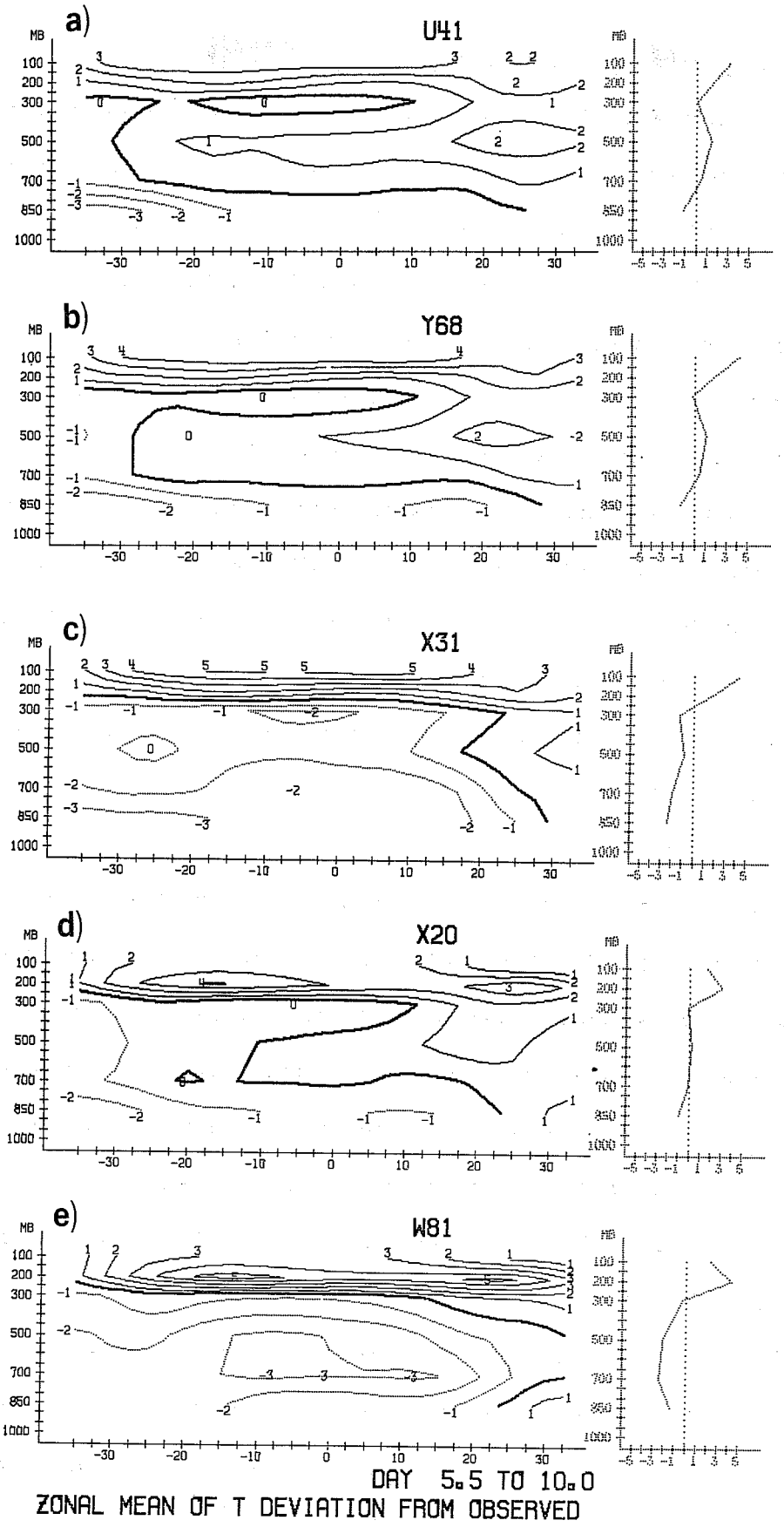

Fig. 10 Height-latitude distribution of days 5-10 means of zonally averaged temperature deviations for the tropical belt (35°S - 32.5°N).

3.2 Impact of the changes on the hydrological cycle

The precipitation maps (Fig. 11) show some marked differences associated with the various changes in the physical processes. The control experiment (W81) is characterised by excessive precipitation over Indonesia and a rather weak ITCZ (Fig. 11(a)) when compared with climatological estimates for June (Fig. 11(f)) from Jaeger (1976). The monsoonal rains over India are also underestimated although it should be remembered that in 1979 the onset of the monsoon was relatively late (around 13 June) rather than at the 'normal' time of May 31. With the introduction of the new radiation code (X31) there is a general reduction in precipitation (Fig. 11(b)) associated with increased atmospheric stability due to a decrease in radiative cooling in the middle troposphere and increase in cooling near the surface as discussed in Section 3.1. Nevertheless the faults in the precipitation pattern remain with an even weaker ITCZ over the Pacific.

The shallow convection and modified Kuo schemes have the greatest impact on the precipitation (X20). Compared to the control (W81), considerably higher precipitation rates occur along the ITCZ downstream of the trades (Atlantic and North Brazil, Central Pacific, Indian Ocean) and smaller rates over Indonesia (Figs. 11(a) and 11(c)). The distribution is now much more realistic when compared with Jaeger's climatology (Fig. 11(f)). However, the monsoon rains over India and the Arabian Sea are still underestimated whilst the maximum in the Somali Jet and north of the Bay of Bengal seem unrealistically large. It is interesting to note that when the radiation changes are added to the convection changes (Y68) there is a marked improvement in these features (Fig. 11(d)) as was evident also in the flow pattern discussed in Section 3.1. The monsoon rains are increased and the

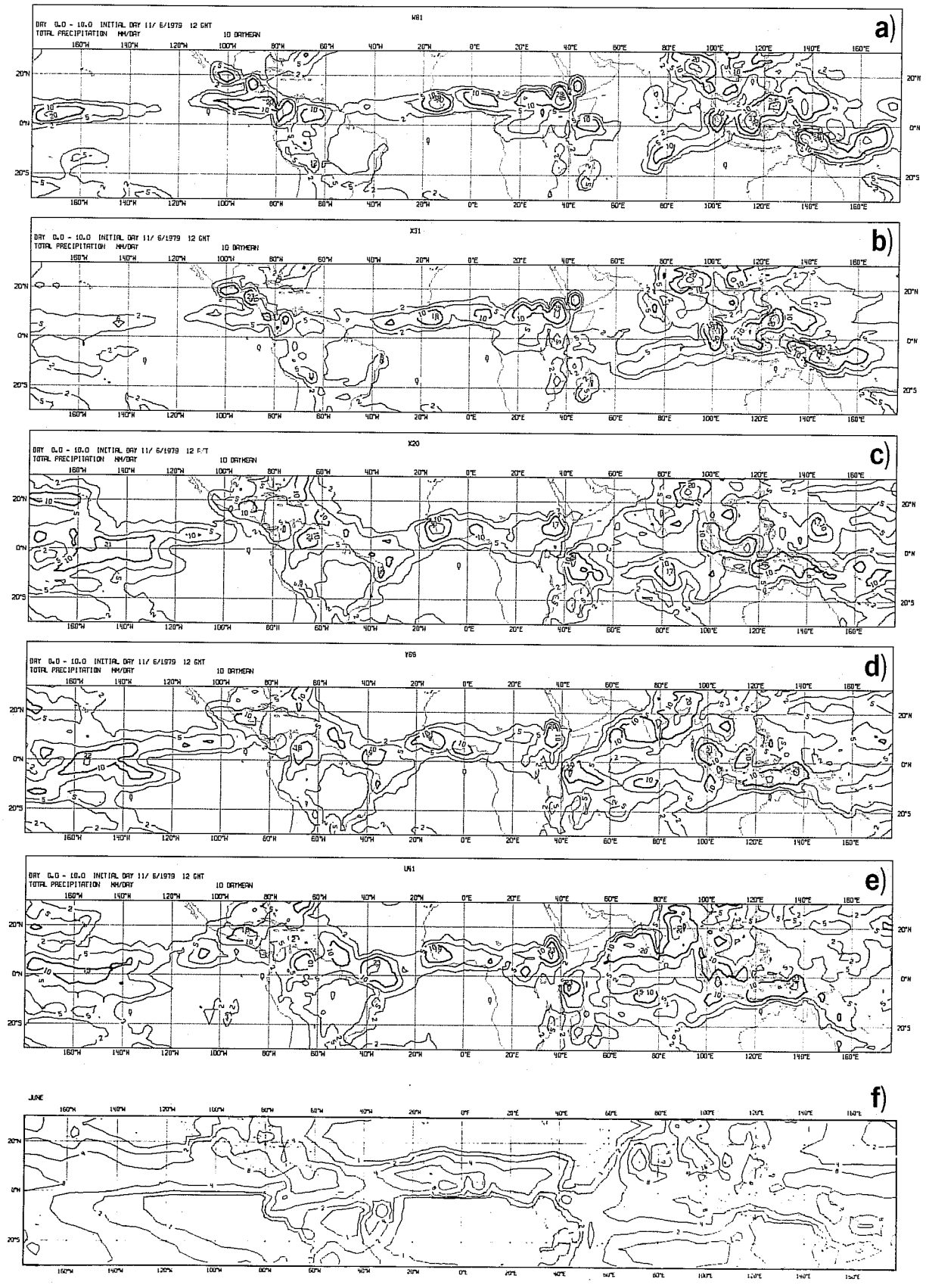

Fig. 11 10 day mean total precipitation rate (mm day^{-1}). (a) W81, (b) X31, (c) X20, (d) Y68, (e) U41 and (f) Jaeger's climate values for June.

Bay of Bengal precipitation is reduced. The maximum off the coast of Brazil, evident in Jaeger's climatology, is also better represented in this experiment. The addition of the new cloud scheme (U41) leads to a further slight improvement (Fig. 11(e)) particularly in the vicinity of the Indian monsoon. Nevertheless, the rainfall in the Bay of Bengal is still excessive and is related to the anomalous northerly low level flow evident in the mean winds at 850mb (Fig. 8). The net horizontal flux of moisture (Fig. 12) shows that the observed convergence of moisture over south west India is not well represented; rather the model preferentially continues the transport of moisture northwards into the Bay of Bengal releasing it as precipitation on the southern edge of the Himalayan plateau (Fig. 11).

The large change in precipitation when the convection changes are introduced appears to be related primarily to the altered structure in the trade winds due to the shallow convection scheme. As noted earlier, the trade wind boundary layer and cloud layer combined are considerably deeper (Fig. 3) and therefore contain a higher amount of moisture, which is primarily advected into the ITCZ. The moisture balance for the trades implies a larger moisture supply through evaporation from the oceans and this is clearly seen in Fig. 13. Compared to the control (W81), the experiment with all the changes (U41) shows increases in evaporation which exceed 50 Wm^{-2} (equivalent to almost 2mm day^{-1} of precipitable water) over large areas. The evaporation is now much closer to climatology as can be seen in Fig. 13(c) where the mean latent heat flux over the oceans for June from Esbensen and Kushnir (1981) is shown.

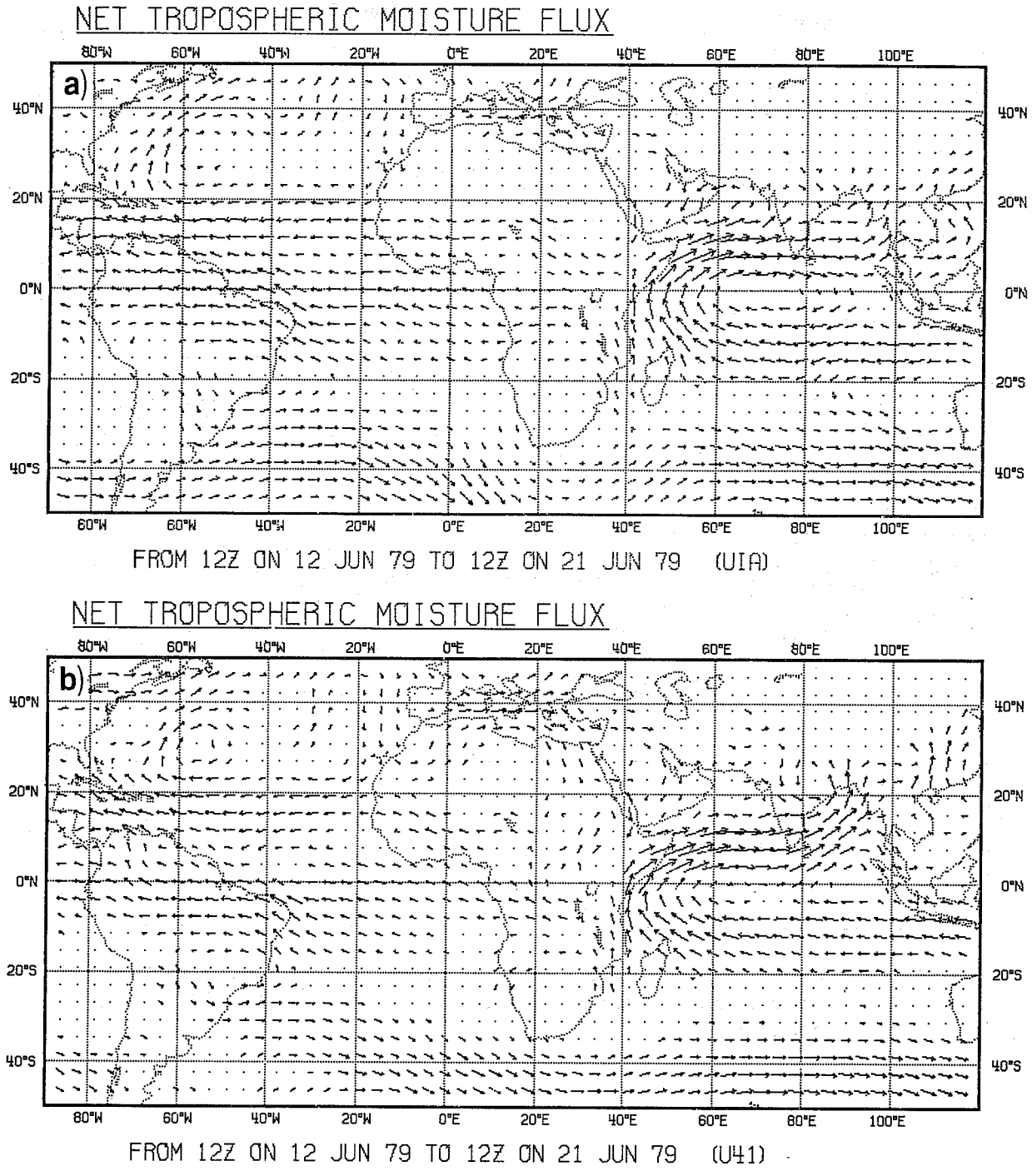

Fig. 12 Days 1-5 mean tropospheric moisture flux (a) observed field, (b) U41.

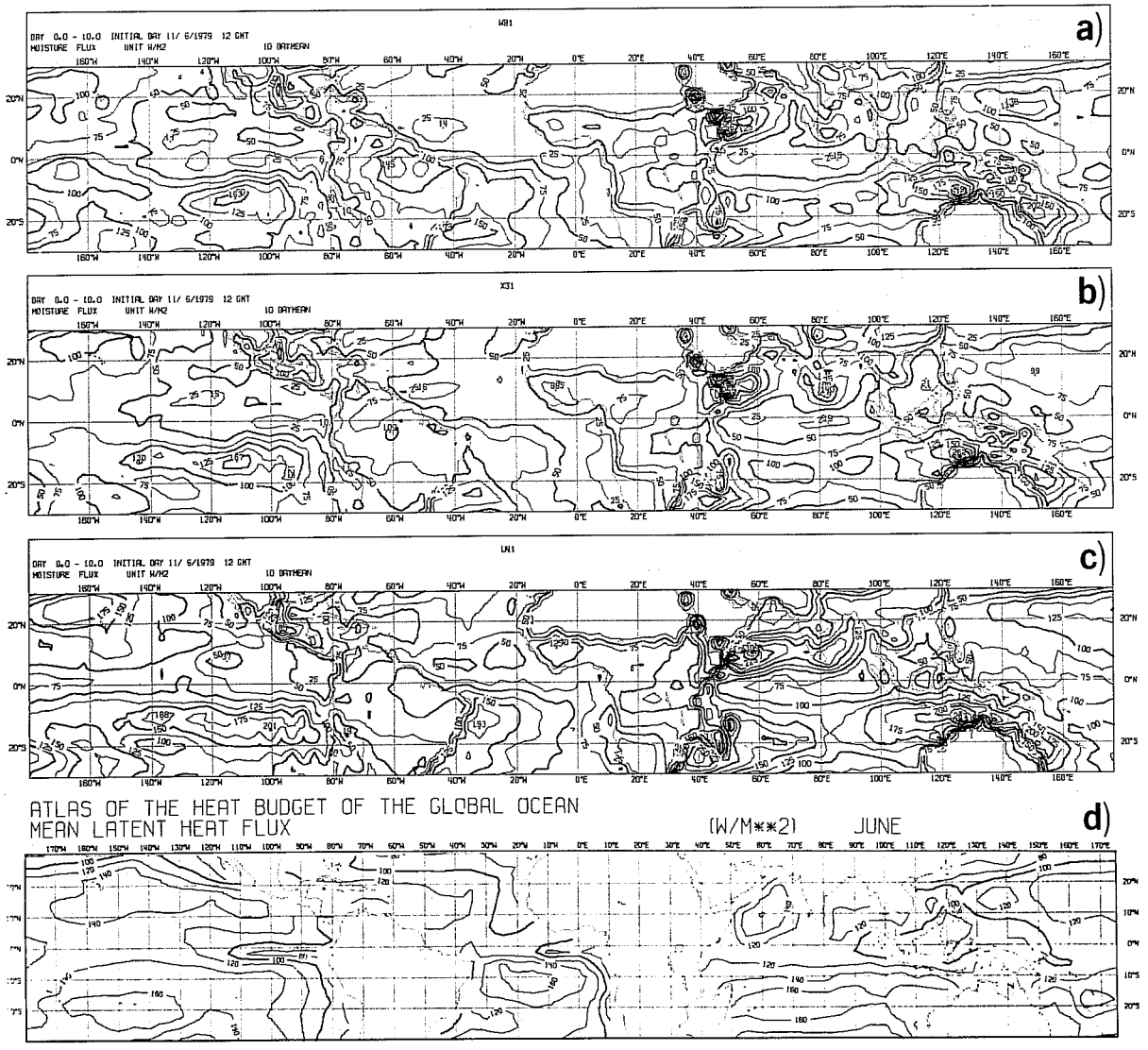

Fig. 13 10 day mean surface evaporation rate (Wm^{-2}). (a) W81, (b) U41, (c) climate values over the ocean for June from Esbensen and Kushnir.

The marked improvement both in the scores and in the simulation of the Indian monsoon which occurs only when the radiation changes are combined with the convection changes is an interesting result of this study. It emphasises that a physical process cannot be considered in isolation. Without detailed diagnostics of the thermal state and physical tendencies over the monsoon region it is not possible to say precisely why this should be so. Unfortunately such diagnostics were not available for these experiments. However, it does seem reasonable to suppose that the poor response of the model to the convection changes only (X20) is due to the unrealistic behaviour of the original radiation scheme in the vicinity of clouds. With the introduction of the shallow convection scheme the vertical temperature and humidity structure has altered so that clouds could be predicted by the original cloud scheme. The well mixed layer restriction in the original cloud scheme (see section 2.2) would cease to operate in areas of shallow convection and cloud would form below the inversion. This difference in vertical structure can be clearly seen in the profiles of Fig. 3. The original radiation scheme would give excessive cooling in response to these clouds, so increasing the strength of the capping inversion and thus restricting the onset of deep convection in the transition regions. With the introduction of the revised radiation scheme the response to these low level clouds would be less pronounced. Again with the new cloud scheme there is a reduction in these clouds, which could account for the further improvement in the occurrence of deep convection in the monsoon region.

3.3 Impact of the changes on the simulation of the Asian summer monsoon

In this section the simulation of the monsoon onset and prediction of the stationary components of the summer monsoon are illustrated. The evolution of the summer monsoon is shown up most dramatically in the rapid intensification of the low-level flow over the Arabian Sea. Time sequences of the kinetic energy (KE) of the 850mb flow over the Arabian Sea region (0°- 22.5°N, 41.25°-75°E) are depicted in Fig. 14. The kinetic energy of the analysed flow shows an increase by about five times between 11 and 17 June. The simulation with all revisions to the physics (U41) clearly performs better than all other experiments. Although in this case KE increases by about 3-4 times between 11-18 June, it still fails to reproduce the observed intensification. The simulation with the modified radiation (X31) performs, to some extent, better than the control (W81), although the growth in KE does not exceed 2-3 times the initial value on June 11. Again as already discussed it can be clearly seen that it is only when the convection changes are combined with the radiation changes (Y68 vs. X20) that some intensification of the flow is simulated. This is consistent with the increased precipitation over the Arabian Sea (Fig. 11) in Y68 and U41, and agrees with other studies (e.g. Krishnamurti et al, 1983; Mohanty et al 1984) which indicate that the intensification of the monsoon flow is mainly determined by the release of convective instability and the development of a diabatic heat source over the Arabian Sea and Indian subcontinent.

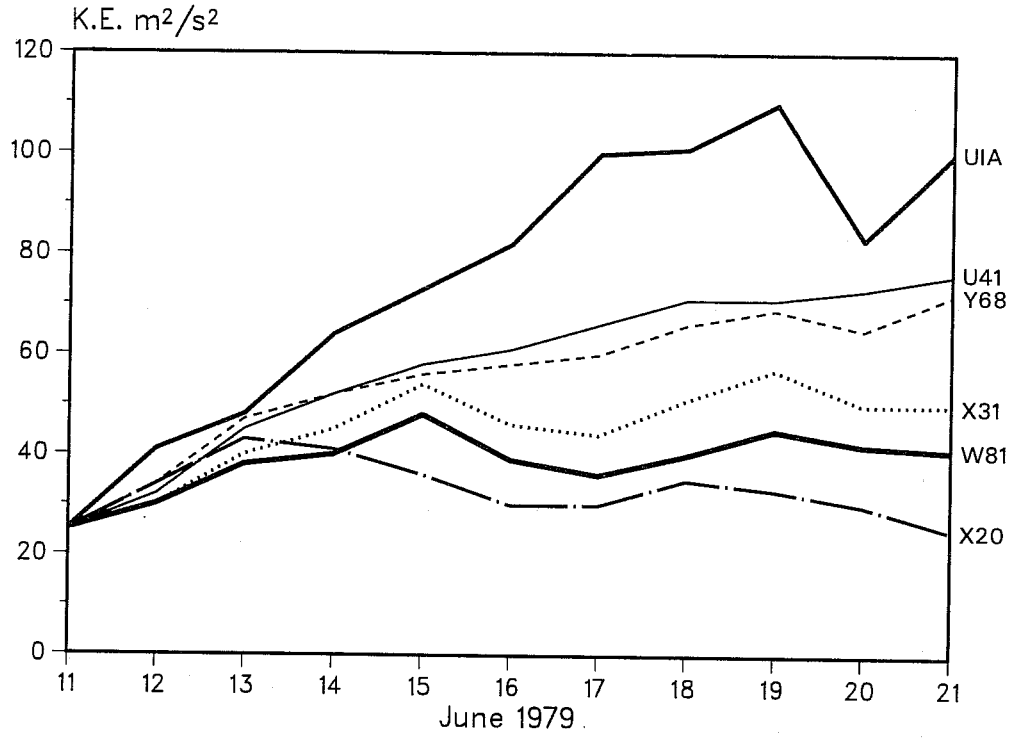

Fig. 14 Time series of the kinetic energy of the 850mb flow over the Arabian Sea region (0-22.5°N, 41.25° - 75°E).

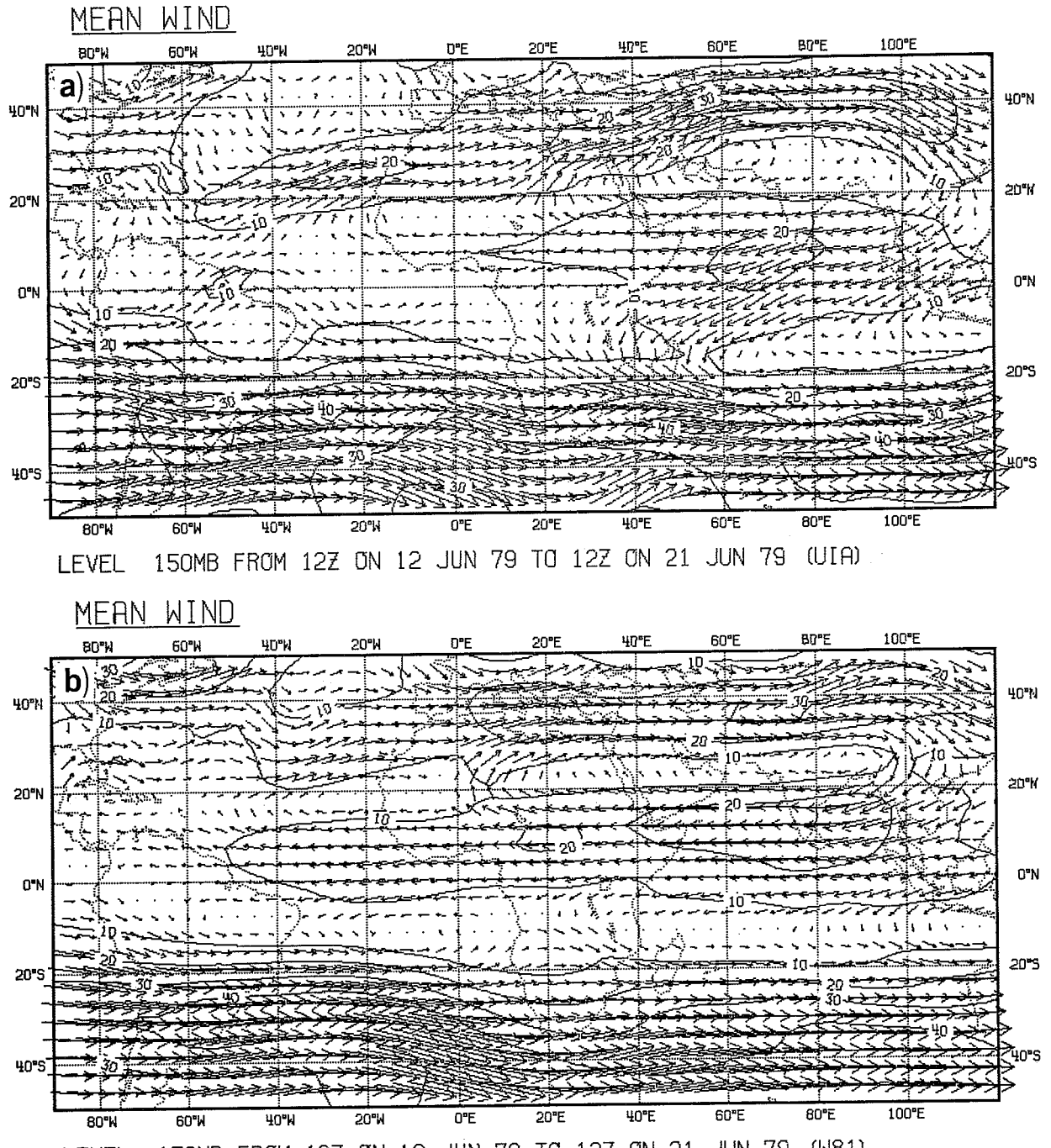

Fig. 15 Days 1-10 mean winds at 150mb. (a) analysed field, (b) W81, (c) X31, (d) U41.

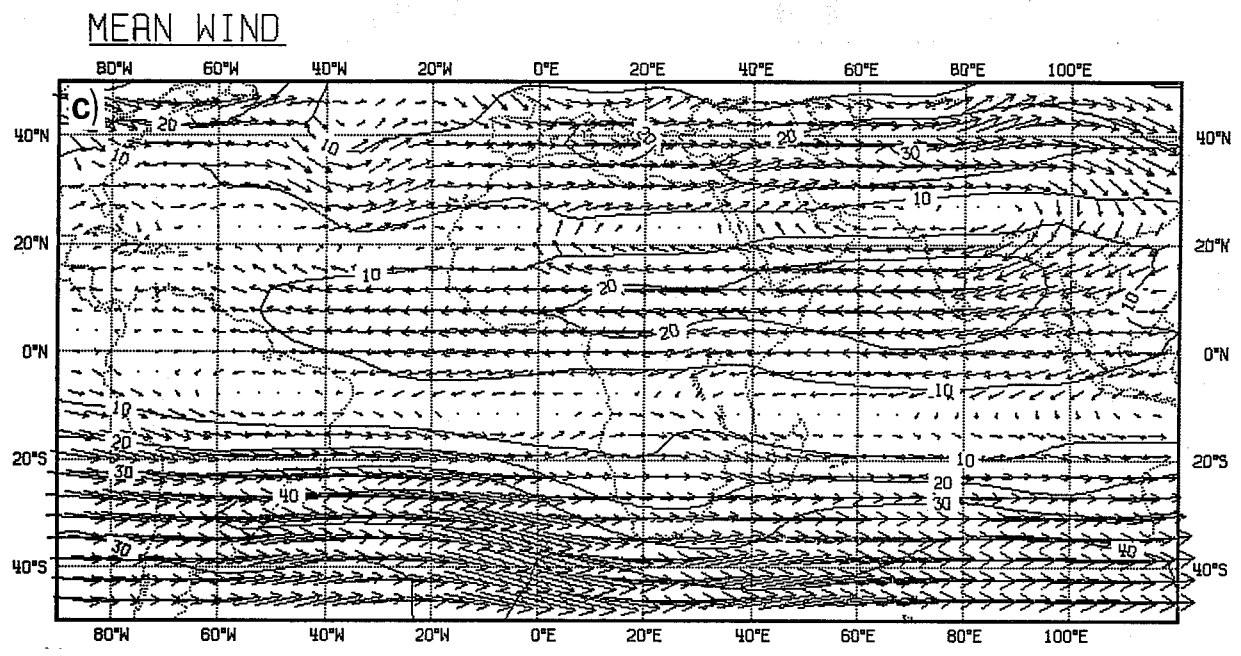
MEAN WIND
c)
80°W 60°W 40°W 20°W 0°E 20°E 40°E 60°E 80°E 100°E
40°N
20°N
0°N
20°S
40°S
LEVEL 150MB FROM 12Z ON 12 JUN 79 TO 12Z ON 21 JUN 79 (X31)

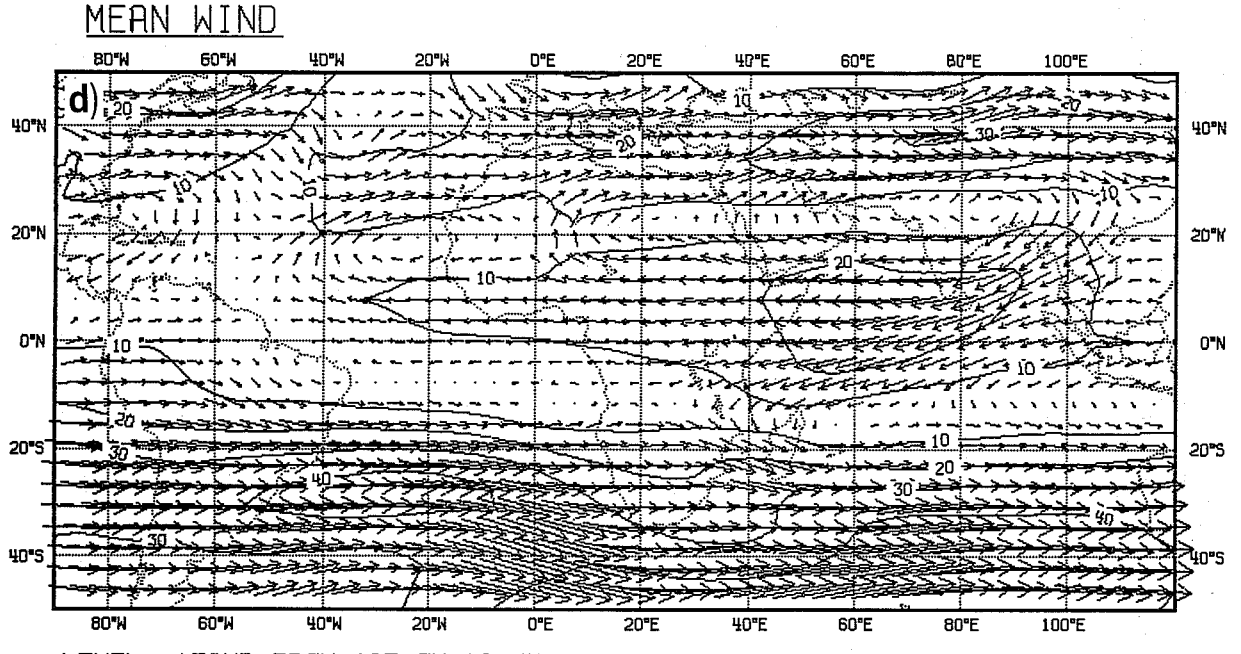
MEAN WIND
d)
80°W 60°W 40°W 20°W 0°E 20°E 40°E 60°E 80°E 100°E
40°N
20°N
0°N
20°S
40°S
LEVEL 150MB FROM 12Z ON 12 JUN 79 TO 12Z ON 21 JUN 79 (U41)

Fig. 15 (contd.)

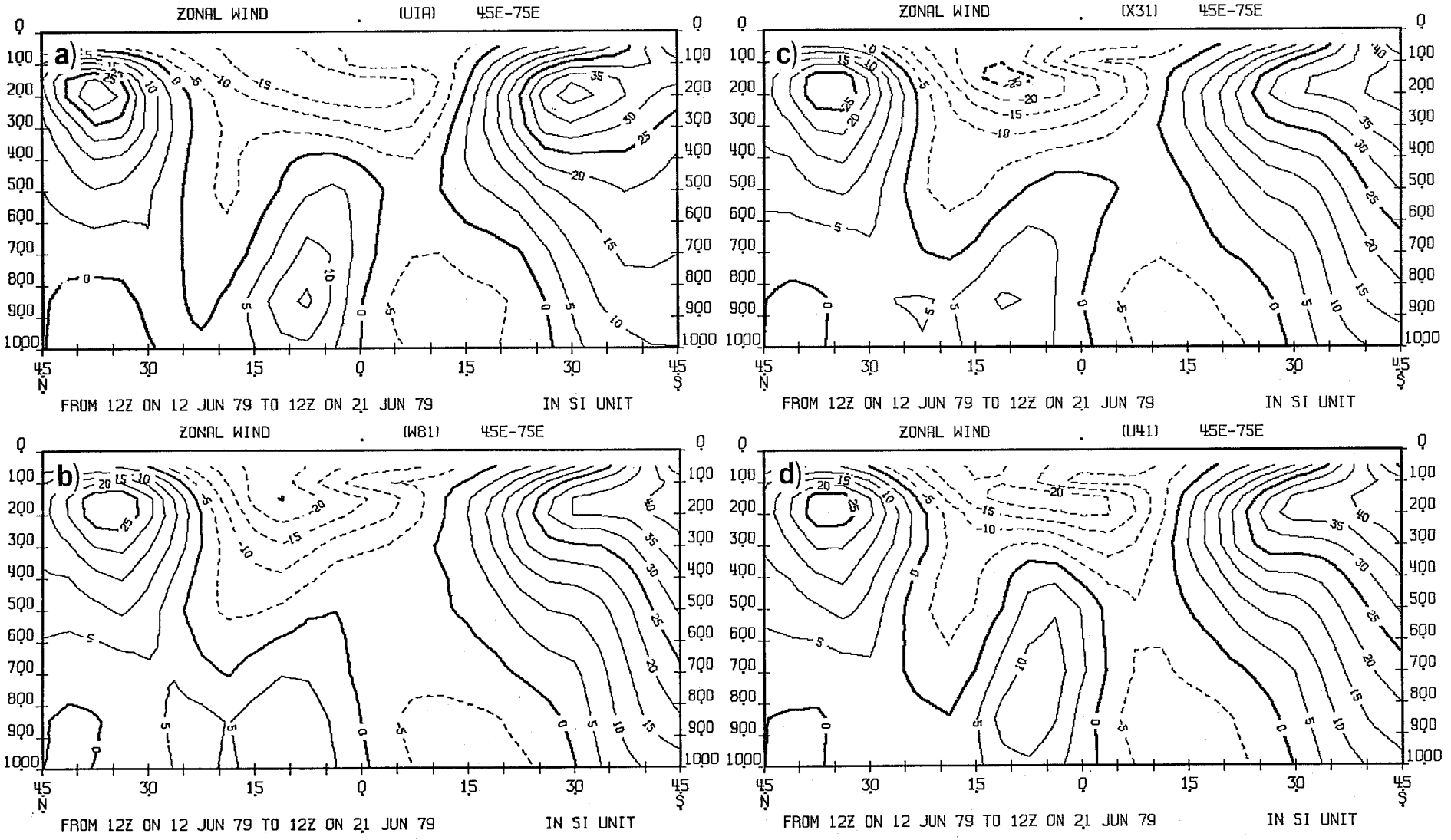

Fig. 16 Days 1-10 mean sectorial average (45° - 75°E) over the Arabian Sea of zonal wind. (a) analysed field, (b) W81, (c) X31, (d) U41.

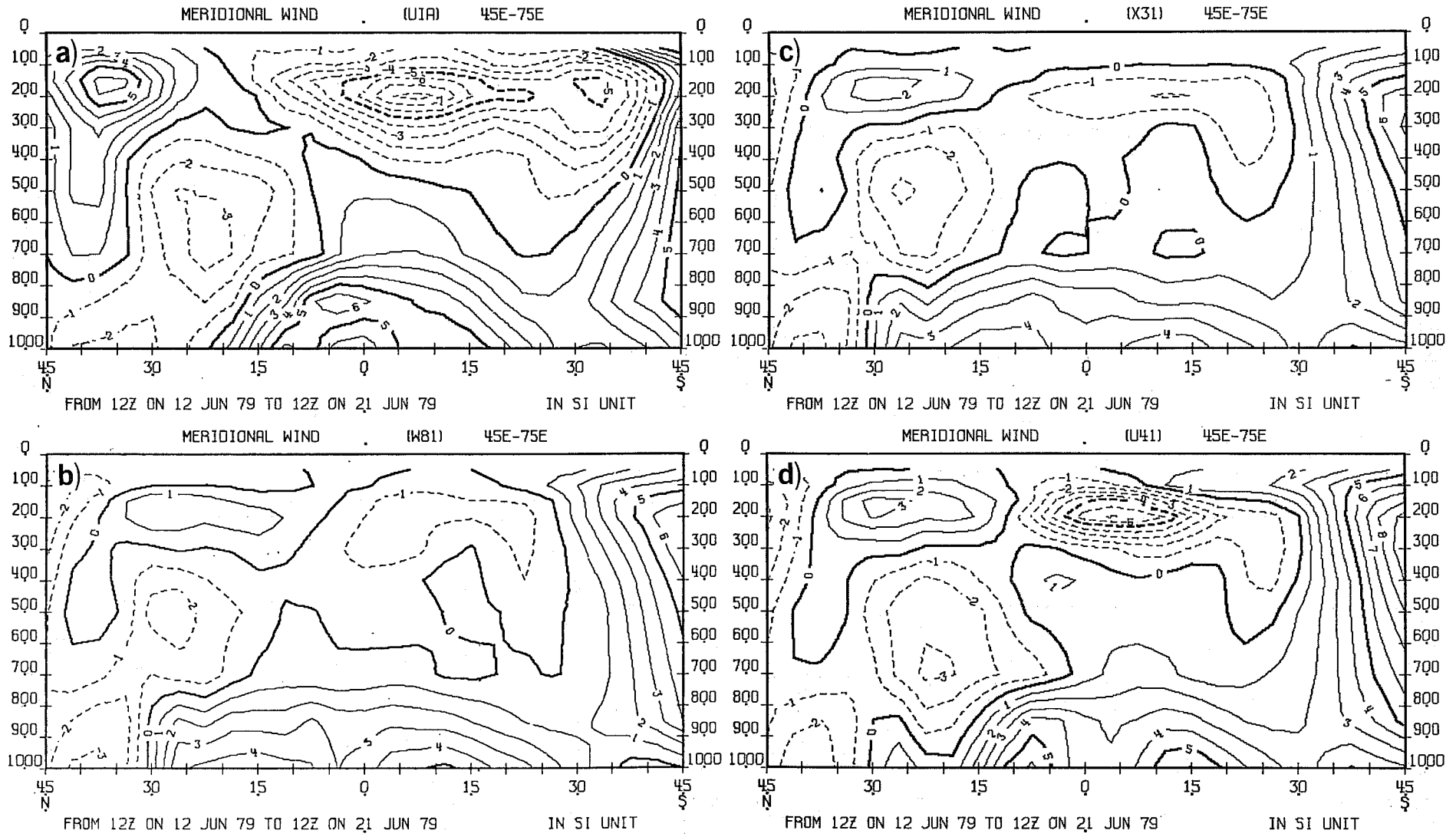

Fig. 17 As Fig. 16 for meridional wind.

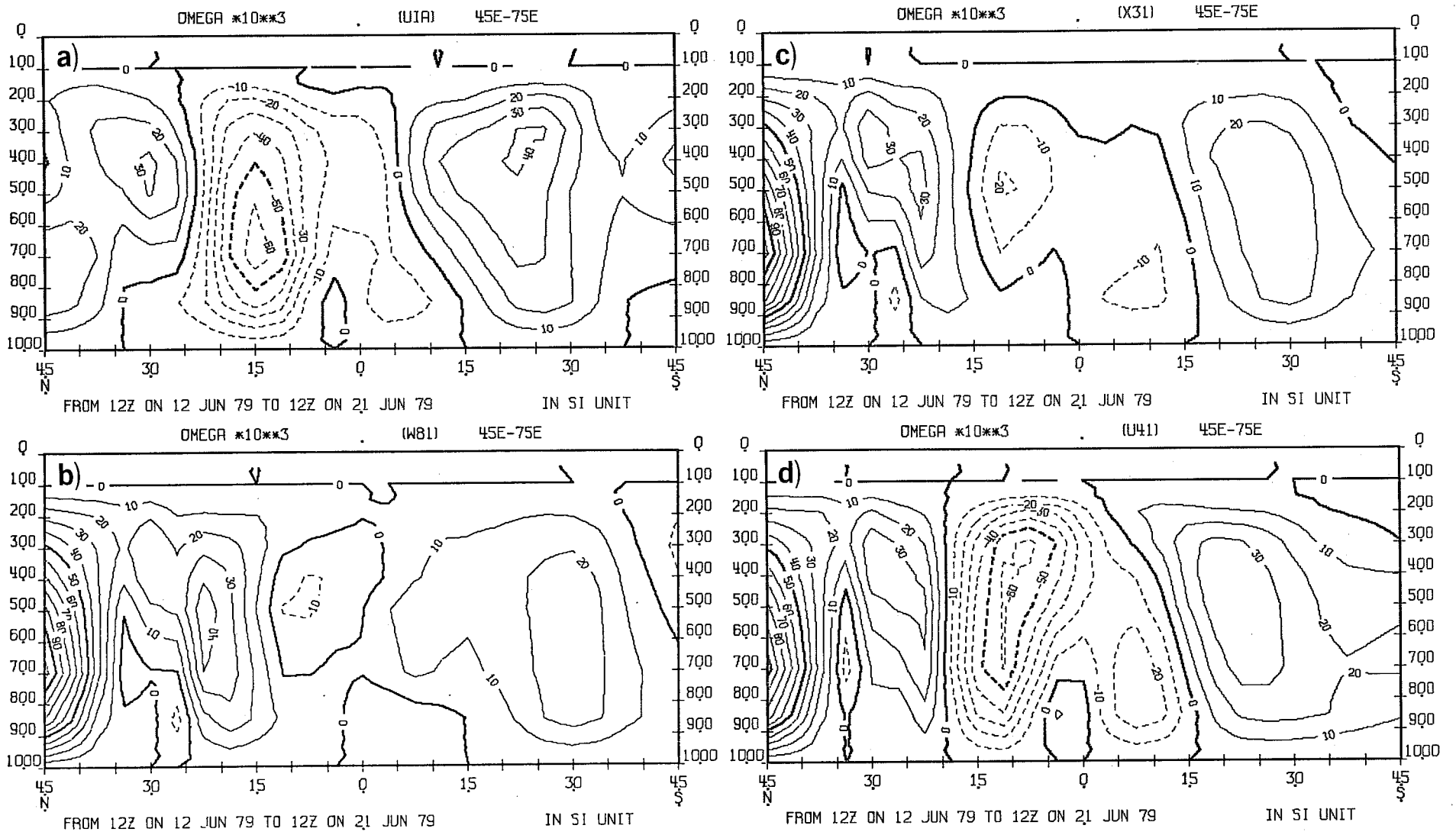

Fig. 18 As Fig. 16 for vertical velocity.

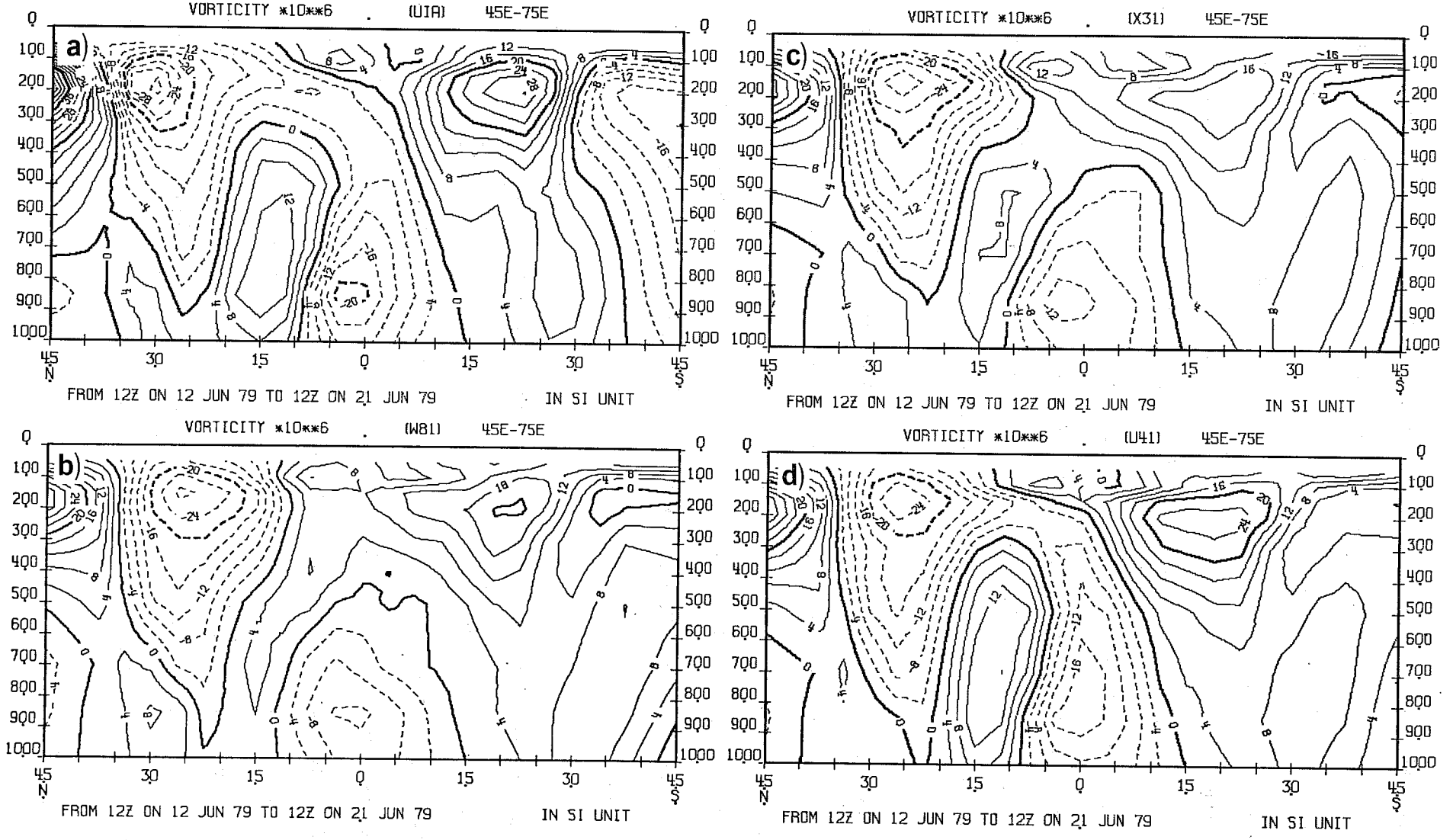

Fig. 19 As Fig. 16 for relative vorticity.

One feature of the onset of the Asian summer monsoon is the development of an upper level cross-equatorial return flow. The time averaged wind fields at 150mb (Fig. 15) show that this pattern is realistically simulated only in experiment U41. Experiments W81 and X31 simulate a strong equatorial zonal flow at 150mb which is considered as a systematic error in operational forecasts. Further, the absence of the upper level divergent flow in W81 and X31 is probably related to the failure of the low-level westerly winds (convergent flow) to intensify over the Arabian Sea. In association with the improved divergent flow over the Indian Ocean in U41 the excessive easterly flow over central Africa and into the Atlantic is greatly reduced.

In association with the development of the monsoon rainfall over the Arabian Sea and India the vertical circulations, driven by the diabatic heating, develop in a characteristic way. The time mean (days 1-10) sectorial averages (45°E - 75°E) over the Arabian Sea of zonal wind (u), meridional wind (v), vertical motion (ω) and relative vorticity (ζ) are shown in Figs. 16-19 respectively.

The observed fields show the southerly cross-equatorial low level flow (Fig. 17(a)) into a strong ascending cell (Fig. 18(a)) associated with the deep convection of the monsoon onset. The return northerly cross equatorial flow is seen in the upper troposphere (Fig. 17(a)). The strong low level westerlies across the southern Arabian Sea are clearly evident in Fig. 16(a). As was seen earlier, only experiment U41 with all the modifications to the physics, reproduces the strong low level westerlies (Fig. 16(d)). Although all experiments show the low level southerly component related to the Somali Jet (Fig. 17), only U41 properly simulates the upper level return northerly

flow as was also evident in Fig. 15. Both experiments W81 and X31 fail to establish the upper tropospheric northerly which is one of the ramifications of the weak monsoon circulation in these experiments. Both the vertical velocity and relative vorticity fields are well represented in experiment U41 (Figs. 18 and 19). This is associated with the development of a substantial area of deep convection in the Arabian Sea (Fig. 11). The poor simulation in experiments W81 and X31 is presumably due to their inability to develop this diabatic heat source. The dramatic improvement in the circulation patterns over the Arabian Sea when all the revisions to the physics are incorporated is a major result of this study.

4. CONCLUSIONS

The changes described in this report constitute a major revision of the physical parameterisation in the model. Apart from the shallow convection, which represents a process not previously parameterised in the model, the other changes are considered as improvements to existing schemes. They are intended to rectify known faults in either the physical concept of the scheme, as is the case with the radiation, or in its performance within the model.

This study has concentrated on the impact of these changes on the medium range weather prediction in the tropics. The results have shown that the combined effect of the changes gives a substantial improvement in the simulation of the tropical tropospheric circulation and hydrological cycle. In particular, the trade winds are much improved as is the precipitation associated with the ITCZ. The erroneous flow over Africa is also largely corrected. These changes can be attributed, in the main, to the introduction of the shallow convection scheme and the modifications to the Kuo deep convection scheme. It was interesting to note however that the radiation changes were necessary for the benefits of the convection changes to be realised. This was particularly evident for the monsoon; without the radiation changes, the convection changes gave no intensification of the monsoon circulation, this being associated with the lack of development of the monsoonal rains over the Arabian Sea and Southern India.

This study also showed the ability of the model, with the modified parameterisation schemes, to predict the upper tropospheric divergent flow over South East Asia and the Indian Ocean. Further, the stationary components of the tropical flow (winds, vertical velocity and relative vorticity) over

the Arabian Sea were remarkably well simulated. However, the model still fails to reproduce fully the explosive growth of the westerlies over the Arabian Sea, and has a tendency to extend the monsoon flow northwards and westwards over India and into the Bay of Bengal. The deficiencies in the model's tropical simulation may be further improved when the four-dimensional data assimulation procedure, which provides the model's initial state, also contains the modifications to the physical processes described in this report.

References

Esbensen, S.K. and Y. Kushnir, 1981: The heat budget of the global ocean. An atlas based on estimates from surface marine observations. Climatic Research Institute. Report No. 29, Oregon State University, Corvallis, Oregon.

Geleyn, J-F. and A. Hollingsworth, 1979: An economical analytical method for the computation of the interaction between scattering and line absorption of radiation. Contr.Atmos.Phys., 52, 1-16.

Jaeger, L., 1976: Monatskarten des Niederschlages für die ganze Erde. Berichte D. Wetterd., Offenbach/Main, Vol.18, No.139, 38pp.

Krishnamurti, T.N., and Y. Ramanathan, 1982: Sensitivity of the monsoon onset to differential heating. J. Atmos. Sci., 39, 1290-1306.

Krishnamurti, T.N., R. Pasch and T. Kitade, 1983: Survey of forecasts starting from a particular SOP-II initial state. WGNE Forecast Comparison Experiments, by C. Temperton, T.N. Krishnamurti, R. Pasch and T. Kitade. Numerical Experimentation Programme Report No. 6, WCRP, WMO, Geneva, 73-104.

Lönnberg, P. and D. Shaw, 1983: ECMWF data assimilation scientific documentation. ECMWF Meteorological Bulletin M1.5/1. Research Manual 1.

Lorenc, A.C., 1981: A global three-dimensional multivariate statistical interpolation scheme. Mon. Wea. Rev., 109, 701-721.

Mohanty, U.C., S.K. Dube and M.P. Singh, 1983: A study of heat and moisture budget over the Arabian Sea and their role in the onset and maintenance of summer monsoon. J. Meteor.Soc. Japan, 61, 208-221.

Mohanty, U.C., R.P. Pearce and M. Tiedtke, 1984: Numerical Experiments on the simulation of the 1979 Asian summer monsoon. ECMWF Tech.Rep. No. 44, 46pp.

Pearce, R.P. and U.C. Mohanty, 1984: Onsets of the Asian summer monsoon 1979-82. J.Atmos.Sci., 41, 1620-1639.

Ritter, B., 1984: The impact of an alternative treatment of infrared radiation on the performance of the ECMWF forecast model. Proceedings of the IAMAP International Radiation Symposium, 21-29 August, Italy (in press).

Simmons, A.J. and M. Jarraud, 1984: The design and performance of the new ECMWF operational model. ECMWF Seminar on Numerical Methods for Weather Prediction, Sept. 5-9, 1983, ECMWF, Reading, U.K., Vol.2, 113-164.

Slingo, J., 1982: Report on a study of the EC radiation scheme, ECMWF Tech. Memo. No. 61, 32pp.

Slingo, J., 1985: Cloud cover experimentation with the ECMWF model. ECMWF Workshop on Cloud Cover and Radiative Fluxes in Large-Scale Numerical Models - Design, Validation and Dynamical Impact (in press).

Slingo, J., and B. Ritter, 1985: Cloud prediction in the ECMWF model. ECMWF Tech. Rep. No.46, 49pp.

Tiedtke, M., 1984: The sensitivity of the time-mean large-scale flow to cumulus convection in the ECMWF model. ECMWF Workshop on Convection in Large-Scale Numerical Models, 28 Nov. - 1 Dec. 1983, Reading, U.K., 297-316.

Tiedtke, M., J-F. Geleyn, A. Hollingsworth and J-F. Louis, 1979: ECMWF Model: Parameterisation of sub-grid scale processes. ECMWF Tech. Rep. No. 10, 46pp.

ECMWF PUBLISHED TECHNICAL REPORTS

No.1 A Case Study of a Ten Day Prediction

No.2 The Effect of Arithmetic Precisions on some Meteorological Integrations

No.3 Mixed-Radix Fast Fourier Transforms without Reordering

No.4 A Model for Medium-Range Weather Forecasting - Adiabatic Formulation

No.5 A Study of some Parameterizations of Sub-Grid Processes in a Baroclinic Wave in a Two-Dimensional Model

No.6 The ECMWF Analysis and Data Assimilation Scheme - Analysis of Mass and Wind Fields

No.7 A Ten Day High Resolution Non-Adiabatic Spectral Integration: A Comparative Study

No.8 On the Asymptotic Behaviour of Simple Stochastic-Dynamic Systems

No.9 On Balance Requirements as Initial Conditions

No.10 ECMWF Model - Parameterization of Sub-Grid Processes

No.11 Normal Mode Initialization for a Multi-Level Gridpoint Model

No.12 Data Assimilation Experiments

No.13 Comparisons of Medium Range Forecasts made with two Parameterization Schemes

No.14 On Initial Conditions for Non-Hydrostatic Models

No.15 Adiabatic Formulation and Organization of ECMWF's Spectral Model

No.16 Model Studies of a Developing Boundary Layer over the Ocean

No.17 The Response of a Global Barotropic Model to Forcing by Large-Scale Orography

No.18 Confidence Limits for Verification and Energetic Studies

No.19 A Low Order Barotropic Model on the Sphere with the Orographic and Newtonian Forcing

No.20 A Review of the Normal Mode Initialization Method

No.21 The Adjoint Equation Technique Applied to Meteorological Problems

No.22 The Use of Empirical Methods for Mesoscale Pressure Forecasts

No.23 Comparison of Medium Range Forecasts made with Models using Spectral or Finite Difference Techniques in the Horizontal

No.24 On the Average Errors of an Ensemble of Forecasts

ECMWF PUBLISHED TECHNICAL REPORTS

No.25 On the Atmospheric Factors Affecting the Levantine Sea

No.26 Tropical Influences on Stationary Wave Motion in Middle and High Latitudes

No.27 The Energy Budgets in North America, North Atlantic and Europe Based on ECMWF Analyses and Forecasts

No.28 An Energy and Angular-Momentum Conserving Vertical Finite-Difference Scheme, Hybrid Coordinates, and Medium-Range Weather Prediction

No.29 Orographic Influences on Mediterranean Lee Cyclogenesis and European Blocking in a Global Numerical Model

No.30 Review and Re-assessment of ECNET - a Private Network with Open Architecture

No.31 An Investigation of the Impact at Middle and High Latitudes of Tropical Forecast Errors

No.32 Short and Medium Range Forecast Differences between a Spectral and Grid Point Model. An Extensive Quasi-Operational Comparison

No.33 Numerical Simulations of a Case of Blocking: the Effects of Orography and Land-Sea Contrast

No.34 The Impact of Cloud Track Wind Data on Global Analyses and Medium Range Forecasts

No.35 Energy Budget Calculations at ECMWF: Part I: Analyses

No.36 Operational Verification of ECMWF Forecast Fields and Results for 1980-1981

No.37 High Resolution Experiments with the ECMWF Model: a Case Study

No.38 The Response of the ECMWF Global Model to the El-Nino Anomaly in Extended Range Prediction Experiments

No.39 On the Parameterization of Vertical Diffusion in Large-Scale Atmospheric Models

No.40 Spectral characteristics of the ECMWF Objective Analysis System

No.41 Systematic Errors in the Baroclinic Waves of the ECMWF Model

No.42 On Long Stationary and Transient Atmospheric Waves

No.43 A New Convective Adjustment Scheme

No.44 Numerical Experiments on the Simulation of the 1979 Asian Summer Monsoon

No.45 The Effect of Mechanical Forcing on the Formation of a Mesoscale Vortex

ECMWF PUBLISHED TECHNICAL REPORTS

No.46 Cloud Prediction in the ECMWF Model

No.47 Impact of Aircraft Wind Data on ECMWF Analyses and Forecasts during the FGGE Period, 8-19 November 1979 (not on WP, text provided by Baede)

No.48 A Numerical Case Study of East Asian Coastal Cyclogenesis

No.49 A Study of the Predictability of the ECMWF Operational Forecast Model in the Tropics

No.50 On the Development of Orographic Cyclones

No.51 Climatology and Systematic Error of Rainfall Forecasts at ECMWF

No.52 Impact of Modified Physical Processes on the Tropical Simulation in the ECMWF Model